

~~CONFIDENTIAL~~UNCLASSIFIED
MAY 1 1952

NACA

RESEARCH MEMORANDUM

COOLING CHARACTERISTICS OF AN EXPERIMENTAL TAIL-PIPE
BURNER WITH AN ANNULAR COOLING-AIR PASSAGE

By William K. Koffel and Harold R. Kaufman

Lewis Flight Propulsion Laboratory
Cleveland, Ohio

CLASSIFICATION CHANGED

FOR REFERENCE

To UNCLASSIFIED

NOT TO BE TAKEN FROM THIS ROOM

By authority of WASA CORP #48 Date 12-29-65

Kme 1-24-66

CLASSIFIED DOCUMENT

This material contains information affecting the National Defense of the United States within the meaning of the espionage laws, Title 18, U.S.C., Secs. 793 and 794, the transmission or revelation of which in any manner to unauthorized person is prohibited by law.

NATIONAL ADVISORY COMMITTEE
FOR AERONAUTICSWASHINGTON
February 26, 1952~~CONFIDENTIAL~~
UNCLASSIFIEDNACA LIBRARY
LANGLEY AERONAUTICAL LABORATORY
Langley Field, Va.

NACA RM E51K23



NATIONAL ADVISORY COMMITTEE FOR AERONAUTICS

RESEARCH MEMORANDUM

COOLING CHARACTERISTICS OF AN EXPERIMENTAL TAIL-PIPE

BURNER WITH AN ANNULAR COOLING-AIR PASSAGE

By William K. Koffel and Harold R. Kaufman

SUMMARY

The effects of tail-pipe fuel-air ratio (exhaust-gas temperatures from approximately 3060° to 3825° R), radial distribution of tail-pipe fuel flow, and mass flow of combustion gas on the temperature profiles of the combustion gas and on temperature profiles of the inside wall of the combustion chamber were determined for an experimental tail-pipe burner cooled by air flowing through an insulated cooling-air passage 1/2 inch in height. The effects on inside-wall temperature of varying the mass-flow ratio of cooling-air to combustion-gas mass flow from approximately 0.067 to 0.19, inlet cooling-air temperature from about 520° to 1587° R, and combustion-gas mass flow from 22.3 to 13.8 pounds per second were also determined.

Large circumferential variations existed in the combustion-gas temperature near the inside wall. These variations resulted in similar variations in the inside-wall temperature. The circumferential variations formed consistent patterns that were similar, although different in magnitude, for all configurations tested.

The two extremes in radial distribution of tail-pipe fuel flow, high fuel concentration toward the combustion-chamber wall and high fuel concentration in the center of the combustion chamber, changed the circumferential average inside-wall temperature 235° F at a station 48 inches downstream of the flame holder. The configuration having a high fuel concentration near the wall presented a more severe cooling problem as the circumferential variation was greatest for this configuration.

The spread of flame to the inside wall, as determined from measurements of combustion-gas temperature near the wall, was practically unaffected by fuel-air ratio. However, the flame spread to the wall was a function of radial fuel distribution. At no time did the flame impinge on the wall within 24 inches downstream of the flame holder. Radiant heat transfer to this section of the inside wall was insufficient to require wall cooling in the first 24 inches, if the tail-pipe materials could withstand nonafterburning operation without cooling.

With the most uniform distribution of tail-pipe fuel tested and an inlet cooling-air temperature of 520° R, an average inside-wall temperature of 1300° F at a station 48 inches downstream of the flame holder required mass-flow ratios of 0.12 and 0.09 with exhaust-gas temperatures of 3825° and 3435° R, respectively. When the distance was increased to 56 inches downstream of the flame holder, a mass-flow ratio of 0.115 was necessary with an exhaust-gas temperature of 3435° R.

At a mass-flow ratio of 0.145, the inside-wall temperature 48 inches downstream of the flame holder was increased about $4/10^{\circ}$ per degree increase in inlet cooling-air temperature.

The temperature of the structural wall of an insulated tail-pipe burner having an inner liner would be practically the same with or without tail-pipe burning.

INTRODUCTION

The combustion-chamber walls of tail-pipe burners must either withstand high operating temperatures or be cooled to temperatures that give adequate strength and service life. The trend toward nonstrategic materials and improvements in performance and the operating range of tail-pipe burners have made cooling more critical. Many methods have been considered for cooling the walls of a tail-pipe combustion chamber including the flow of air through an annular passage surrounding the combustion chamber, the flow of turbine outlet gas through an annular passage formed by a concentric inner liner, the establishment of a cool-air film between the walls and the combustion gas by means of a porous wall or a series of annular nozzles, as well as ceramic coatings and fuel additives that coat the walls and reduce the radiant heat transfer to the walls or lower the wall temperature by their insulative properties. Many combinations of these methods have been and are being investigated at the NACA Lewis laboratory. Considerable attention has been given to the annular cooling-air shroud and to the inner liner and to their use in combination.

An analytical method was developed (reference 1) for calculating the maximum average wall temperature in tail-pipe combustion chambers cooled by the parallel flow of air through an annular cooling passage or cooled by turbine discharge gases flowing between an inner liner and the combustion-chamber wall. The method was based on the simplifying assumptions of a uniform transverse temperature profile, a linear rise in combustion-gas temperature from flame holder to exhaust-nozzle exit, and the fact that radiation from the combustion gas to the wall was twice the nonluminous radiation of a completely burned stoichiometric mixture of octane and air. Wall temperatures or cooling-air flows calculated by the method of reference 1 have checked well with values

measured on experimental tail-pipe burners in which a uniform transverse temperature profile was approached. Agreement was poorer for burners producing nonuniform profiles. Some effects of changing the flameholder design and tail-pipe fuel distribution, and consequently the transverse temperature profile, are given in reference 2.

The cooling and pumping characteristics of a tail-pipe burner having an inner liner and an external cooling-air shroud with an ejector nozzle are presented in reference 3, and an analytical method is developed in reference 4 for predicting the pressure drop through the cooling passages. These investigations on tail-pipe-burner cooling had limited ranges of cooling-air flows and inlet cooling-air temperature and no attempt was made to determine the combustion-gas temperature profiles as effected by changes in internal configuration and to relate them to the temperatures of the combustion-chamber walls.

This report includes some results of an experimental investigation on a tail-pipe burner which was extensively instrumented. Ranges of independent control of the cooling-air temperature, flow, and pressure, as well as the combustion-gas temperature and flow wider than those given in the references are presented herein. The data presented were obtained with a combustion chamber having a constant-flow area and an annular cooling passage of constant height. The effects of exhaust-gas temperature level, distribution of tail-pipe fuel across the turbine annulus, and mass flow of combustion gas on the temperature profiles of both the combustion gas and the inside wall are presented.

APPARATUS

Engine

A conventional and axial-flow turbojet engine was used in this investigation. The sea-level static thrust of the engine was approximately 3100 pounds at a rated engine speed of 12,500 rpm and a maximum turbine-outlet temperature of approximately 1200° F (1660° R). At this condition the air flow was slightly less than 60 pounds per second.

The fuel used in the engine and the tail-pipe burner was MIL-F-5572, grade 80, unleaded gasoline and had a lower heating value of 19,000 Btu per pound and a hydrogen-carbon ratio of 0.185.

Installation

The standard tail pipe was replaced by an experimental tail-pipe-burner assembly attached to the turbine flange. The engine and the tail-pipe burner were mounted on a wing section in the 20-foot-diameter

test section of the altitude wind tunnel. Refrigerated air was supplied to the compressor inlet through a duct from the tunnel make-up air system. This duct was connected to the engine with a labyrinth seal, which made possible measurement of thrust with the tunnel balance system. Air was throttled from approximately sea-level pressure to the desired pressure at the compressor inlet; while pressure in the tunnel test section was maintained at the desired altitude. Cowlings and fairings were omitted from the engine and the tail-pipe burner in order to simplify the installation and to facilitate inspection and servicing of engine, tail-pipe burner, and instrumentation.

2408

Tail-Pipe-Burner Assembly

The entire tail-pipe-burner assembly was fabricated of 1/16-inch Inconel. The over-all length of the engine and tail-pipe burner was approximately 16.1 feet, of which the tail-pipe diffuser, the combustion chamber, and the nozzle were 2, 5, and 1 feet, respectively. Figure 1 is a schematic drawing of the installation showing the fuel-spray bars in the annular diffuser, the cylindrical combustion chamber with insulated cooling passage, and the fixed-conical exhaust nozzle. The flame holder had a single V-gutter with sinusoidal corrugations on the trailing edges. The V-gutter had a mean diameter of 18 inches, a mean width across the corrugations of $1\frac{3}{4}$ inches, and an included angle of 35° . The blockage at the downstream face of the flame holder was about 23 percent and the velocity at the flame holder under the conditions of this investigation was approximately 480 feet per second. The cooling passage had a constant height of 1/2 inch and was insulated with 1 inch of refractory cement.

Fuel-spray bars. - Twelve radial fuel-spray bars were equally spaced 8.75 inches downstream of the turbine flange and 13.25 inches upstream of the flame-holder center line. Each bar had seven holes (number 76 drill) that sprayed fuel normal to the gas flow. Three different sets (twelve bars per set) of spray bars were used to vary the fuel distribution across the turbine discharge annulus. The first set (fig. 2(a)) produced a nearly uniform fuel distribution with a slightly higher fuel concentration at the very center for flame stability and piloting action. The second set (fig. 2(b)) increased the fuel concentration toward the combustion-chamber wall and decreased the fuel flow in the center of the combustion chamber. The third set of spray bars (fig. 2(c)) concentrated more fuel at the center and decreased the fuel concentration near the combustion-chamber walls.

Configurations. - The three sets of fuel-spray bars were used in combination with four different exhaust nozzles to form essentially three configurations as follows:

Configuration	Fuel-spray bars	Exhaust-nozzle exit area (sq ft)	Figure
A	Set 1	1.846 1.903 1.980 2.160	3(a)
B	Set 2	1.903	3(b)
C	Set 3	1.903 2.160	3(c)

INSTRUMENTATION

Because it was recognized that the combustion pattern would be irregular and the temperatures to be measured were severe on thermocouples, as many thermocouples as practicable were used in order to obtain representative average temperatures and to provide sufficient thermocouples if some thermocouples should fail. Six instrumentation stations, B to G (fig. 3), were provided along the length of the cylindrical combustion chamber. Thermocouples were installed at station B for measurement of the inlet cooling-air temperature. Stations C to F had six groups of instrumentation, equally spaced around the circumference, for measuring the temperatures of the inside and outside walls of the tail-pipe burner and of the cooling air as well as the static and total pressures of the cooling air. The temperatures of the inside and outside walls were also measured at four points around the circumference at station G, and the cooling-air temperatures and pressures at station G were measured in the discharge ducts on the downstream plenum chamber. The locations of the instrumentation at each of these stations, at the exhaust nozzle, the cooling-air metering nozzle, and the upstream plenum chamber are shown in figure 4. The cross section of a typical group of instrumentation at stations C through F is shown in figure 5.

The means of providing for longitudinal movement due to thermal expansion can be seen in figure 5. The platinum-rhodium - platinum thermocouple probes extended through sliding seals in the outside wall and the sliding channels connecting the inside and outside walls permitted longitudinal movement of the walls.

The usual pressure and temperature instrumentation was installed at several measuring stations through the engine. Fuel flows to the engine and tail-pipe burner were measured with calibrated rotameters.

Wall-temperature measurement. - The temperature of the inside wall of the tail-pipe burner was measured with chromel-alumel thermocouples spot-welded to the outer surface of the wall (fig. 5). Conductive

cooling of the junction was reduced by strapping the leads to the wall for 3/4 inch downstream of the junction before extending the leads across the cooling passage. The temperature of the outside wall was measured by a chromel-alumel thermocouple welded into the head of a hollow oval-headed screw (fig. 5). Conductive cooling of the junction was negligible because the stem of the screw was buried under the cooling-passage insulation.

Cooling-air temperature measurement. - The cooling-air temperatures were measured by means of National Bureau of Standards type (fig. 6) shielded thermocouples (reference 5). The radiation shield consisted of a 1/4-inch length of 1/8-inch silver tubing which was slid over the bare junction and compressed to a biconvex airfoil section.

Combustion-gas temperature measurement. - Combustion-gas temperatures near the inside wall were measured by means of the platinum-rhodium - platinum thermocouples shown in figure 7. Each thermocouple probe had a water-cooled supporting stem and two thermocouples in parallel having a common hot junction. The leads from the junction were arranged in a cross to give mechanical support at high temperatures. Negligible conduction error was obtained by means of the high length-diameter ratio of the leads between the junction and the cooled supporting stem. No radiation shield was used because of the low emissivity and absorptivity of the platinum and platinum-rhodium wires.

Gas temperature profiles at station F were obtained by means of a rake having seven sonic-flow orifice temperature probes (fig. 8). The temperature of a gas sample flowing into one of these probes is obtained from a thermodynamic equation and is theoretically independent of radiation effects (see reference 6).

The exhaust-gas temperature was computed (as given in appendix A) from rake measurements of total pressure at the exhaust-nozzle exit and the measured gas flow.

Accuracy

Four flight recorders were used because of the large number of thermocouples and in order to reduce the recording time while maintaining equilibrium conditions. The estimated over-all accuracy of the temperature measurements are as follows:

Wall temperature, °F	±15
Cooling air, °F	±10
Gas temperatures near the wall, °F	±20
Sonic-flow orifice probe, °F	±150
Exhaust gas temperature, °F	±50

~~CONFIDENTIAL~~

The geometry of the tail-pipe diffuser and the flame holder in combination with the fuel-spray bars producing approximately uniform distribution of fuel across the turbine annulus (configuration A) was shown, in preliminary tests on a similar burner, to give good performance and operating characteristics over a wide range of altitudes and fuel-air ratios. Cooling characteristics of the experimental tail-pipe burner were obtained with the seven combinations of exhaust-nozzle exit area and fuel-spray bars, at pressure altitudes of 30,000 and 40,000 feet, a flight Mach number of 0.52, and an engine speed of 12,500 rpm. It was impossible to run the tests at lower pressure altitudes because the flow of dry cooling air, at approximately atmospheric pressure from outside the tunnel, was dependent on the difference in the atmospheric pressure and the pressure in the tunnel test section. Dry refrigerated air was supplied to the engine at $505 \pm 5^\circ$ R. The total pressure at the engine inlet was regulated to correspond to the desired pressure at each altitude with complete free-stream total-pressure recovery.

Most of the data were obtained by adjusting the tail-pipe fuel flow to maintain an average turbine-outlet temperature of $1633^\circ \pm 12^\circ$ R; an approximately constant exhaust-gas temperature was thus obtained for each nozzle-exit area and mass flow. The remainder of the data were taken at lower turbine-outlet temperatures.

The cooling-air flow and the cooling-air temperature were systematically varied while holding all other quantities constant.

The approximate range of variables investigated with a limiting turbine-outlet temperature of 1633° are given in the following table:

Configuration	Altitude (ft)	Exhaust-gas temperature T_g ($^{\circ}R$)	Combustion-gas flow W_g (lb/sec)	Mass ratio W_a/W_g	Cooling-air inlet temperature T_a ($^{\circ}R$)
A	30,000	3060	22.1	0.0672 to .1872	500 to 1587
	30,000	3240	22.2	0.1002 to .1917	500 to 1222
	30,000	3435	22.3	0.0953 to .1796	502 to 1408
	40,000	3265	13.8	0.1440	528 to 1340
	30,000	3825	22.8	0.1374 to .1906	515
B	30,000	3215	22.2	0.0985 to .1891	495 to 1223
C	30,000	3235	22.3	0.1420	524 to 1450
	30,000	3764	22.4	0.1912	524

The cooling-air mass flow was controlled by flap valves on the outlet ducts of the downstream plenum chamber. The static pressure in the cooling passage was balanced against the static pressure of the combustion gas at station F by means of pressure-regulating valves upstream of the air-metering nozzle in conjunction with the flap valves. When the pressures were balanced, large pressure forces were transferred from the hot, and consequently weaker, inside wall to the cooler outside wall. This transfer tended to minimize any changes in cooling-passage height. The cooling-air temperature was varied by means of a turbojet can-type combustor in the cooling-air supply duct downstream of the air-metering nozzle.

RESULTS AND DISCUSSION

Typical results of this cooling investigation are presented graphically and the performance of the three configurations are tabulated in

tables I and II. The effects of exhaust-gas temperature level, radial distribution of tail-pipe fuel flow, and combustion-gas mass flow on the temperature profiles of the combustion gas are presented first because of the influence these profiles have on the temperatures of the inside wall.

Reproducibility of Combustion-Gas Temperature Profiles

Circumferential profiles. - The combustion-gas temperatures near the inside wall, the temperature of the inside and outside walls of the cooling passage and the cooling-air temperature are plotted against the group positions around the circumference at station F in figure 9. The reproducibility of the data is indicated in figures 9(a) to 9(c) for a check point having an exhaust-gas temperature of approximately 3060° R, mass-flow ratio of 0.098, and an inlet cooling-air temperature of 530° R. The profiles are similar as the accumulated afterburner time increased from 32 minutes to 9 hours and 22 minutes. The profiles with an exhaust-gas temperature of 3484° R (fig. 9(d)) are similar although the temperature levels are higher. The profiles shown in figure 9 were obtained with the first set of fuel bars, which produced the most uniform fuel distribution. The reproducibility shown is typical of data obtained with the other configurations. The large variations in gas temperatures around the circumference are reflected in the inside-wall temperature. The difference between the highest and the lowest gas temperatures around the circumference, as measured by the platinum thermocouples at station F, was approximately 500° to 900° F, and the difference for the inside-wall temperatures was about 400° to 600° F. The larger circumferential variations in gas temperature are believed to be caused by asymmetrical distributions in the engine fuel-air ratio and in turbine-discharge gas flows because daily inspections disclosed no plugging of the fuel-spray bars in the tail-pipe burner.

Longitudinal profiles. - Typical longitudinal profiles of the combustion-gas temperature measured by the platinum-rhodium - platinum thermocouples $1/2$ inch from the inside wall are shown in figure 10. The general reproducibility of the combustion pattern for a given set of fuel-spray bars can be seen by comparing the relative positions of the temperature profiles for each circumferential group as the exhaust-gas temperature is increased (fig. 10). Similar reproducibility of the relative positions of each group was observed in the longitudinal profiles for the combustion-gas temperature measured $1/4$ inch from the inside wall and for the temperature of the inside wall.

Inasmuch as the longitudinal temperature profiles for various circumferential positions reproduced in a consistent manner in spite of large circumferential temperature variations, the effects of exhaust-gas temperature, of fuel distributions, and of combustion-gas mass flow are based on circumferential average temperatures. (The temperatures in table II are circumferential averages.)

Effect of Variables on Average Longitudinal Profiles
of Combustion-Gas Temperature

Exhaust-gas temperature. - The effect of increased exhaust-gas temperature (or tail-pipe fuel-air ratio) and the spread of the flame toward the inside wall are shown in figure 11. The combustion-gas temperature within 1/4 inch of the wall (fig. 11(a)) remains at approximately turbine-discharge temperature as far downstream as station D indicating that, for the same fuel distribution, the spread of the flame toward the inside wall is practically unaffected by fuel-air ratio (exhaust-gas temperature level) although the transverse temperature gradients between stations C and D increase with fuel-air ratio as can be seen from figure 11(b). Consequently, no cooling would be required for configuration A in the first 24 inches downstream of the flame holder if the burner walls could withstand the nonafterburning operation without cooling. Downstream of this point, the cooling requirements increase as the transverse gas temperature gradients near the wall increase with both distance from the flame holder and with exhaust-gas temperature level.

Fuel distribution. - The effects of marked changes in tail-pipe fuel distribution across the turbine-discharge annulus on the gas temperatures near the inside wall are shown in figure 12. Figure 12(a) shows that the flame spreads out to the wall between 24 and 36 inches downstream of the flame holder depending on the radial distribution of fuel. The flame intercepted the wall first with configuration B, which had a high fuel-air ratio near the wall, and last with configuration C, which had a high fuel-air ratio in the center of the burner. The cooling problem apparently can be altered by changes in fuel distribution at a given exhaust-gas temperature level. It is not, however, always possible to alleviate the cooling problem by altering the radial distribution of fuel because of possible adverse effects on performance and operational characteristics of the tail-pipe burner. For example, configuration C produced low inside-wall temperatures with the third set of fuel-spray bars, and had very smooth combustion and the exhaust nozzle was colder than for configuration A at the same exhaust-gas temperature, but it was impossible to obtain a turbine-outlet gas temperature of 1633° R with these fuel-spray bars when the exhaust-nozzle exit area was 2.160 square feet. On the other hand, configuration B, which produced high inside-wall temperatures, was difficult to ignite, burned roughly, and blew-out whenever the turbine-outlet gas temperature dropped below 1615° R.

The corresponding changes in transverse temperature profiles with changes in fuel distribution will be discussed in the section Fuel Distribution.

Combustion-gas mass flow. - The effect of decreasing the combustion-gas mass flow on the gas temperatures near the inside wall is shown in

2408

figure 13. The decrease in mass flow of combustion gas from 22.29 to 13.85 pounds per second, resulting from increasing the altitude from 30,000 to 40,000 feet, lowered the combustion-gas temperatures between stations E and F, about 400° and 200° F at distances from the inside wall of 1/4 and 1/2 inch, respectively. These temperature reductions, however, would be about one-half as great if cross-plotted data from figure 11 were used to estimate the longitudinal temperature profile at the same exhaust-gas temperature as with the lower mass flow. The decrease in exhaust-gas temperature occurred because the tail-pipe fuel flow was adjusted for a constant indicated turbine-outlet gas temperature, but the mean turbine-outlet gas temperature decreased because of a change in the radial temperature profile as altitude was changed.

Variation of Gas Temperatures Near the Wall with Cooling-Air Flow and Temperature

The temperature of the combustion gas near the wall was affected slightly by the inside-wall temperature, and consequently, by the mass flow and the temperature of the cooling air. The influence of cooling-air flow and the inlet cooling-air temperature on the gas temperature measured 1/4 inch from the inside wall was found to be negligible at stations C and D. The effect of cooling-air flow at stations E and F is given by the approximate equation

$$\Delta T_{g,1/4} = 1000 \Delta \left(\frac{W_a}{W_g} \right) \quad (1)$$

and the effect of inlet cooling-air temperature is about 1/10° per degree rise in inlet cooling-air temperature. (The symbols used are defined in appendix B.)

Effects of Variables on Transverse Gas- Temperature Profile at Station F

Some of the more representative transverse profiles of the combustion-gas temperature at station F were selected for presentation. The temperatures in the combustion zone were obtained by means of the sonic-flow orifice rake and the temperatures near the wall were measured by the platinum-rhodium - platinum thermocouples 1/4 inch from the inside wall.

Exhaust-gas temperature. - Transverse temperature profiles are shown for configuration A in figure 14. Temperature peaks in figure 14(a) corresponding to the wake of the single-V flame holder tend to disappear and the profile to become more uniform as the exhaust-gas temperature is increased (figs. 14(b) and (c)).

The gas temperatures 1/4 inch from the inside wall and in the center of the combustion zone increased 600° to 700° R as the average exhaust-gas temperature increased approximately 440° R.

Fuel distribution. - The effects of changing the radial distribution of fuel across the turbine annulus on the transverse profile of combustion-gas temperature are shown in figure 15. Figure 15(a) shows that the transverse temperature profile of configuration A at an exhaust-gas temperature of 3266° R had a temperature peak in the wake of the flame-holder gutter similar to the peaks existing at an exhaust-gas temperature of approximately 2926° R (fig. 14(a)). The high fuel concentrations near the inside wall in configuration B (fig. 15(b)) resulted in much higher gas temperatures near the inside wall at the bottom of the burner and the gas temperature at the center of the burner was greatly reduced because the tail-pipe fuel-air ratio and exhaust-gas temperatures were practically constant. The average gas temperatures 1/4 inch from the inside wall were approximately 400° R higher for configuration B than for configuration A at a mass-flow ratio of 0.143 and an exhaust-gas temperature of approximately 3240° R. The fuel distribution of configuration C moved the peak temperatures toward the center of the burner and the average gas temperature 1/4 inch from the inside wall was about 350° R lower than for configuration A at a mass-flow ratio of 0.143. For the three radial fuel distributions tested, the increase in fuel concentration in the center of the burner produced a slightly smaller effect on the gas temperatures near the inside wall than did the increase in the fuel concentration toward the walls. This fuel distribution also aggravated the circumferential temperature variations. The relation of these profiles to the average inside-wall temperature will be discussed in the next section.

Effect of Variables on Longitudinal Profiles of Average Inside-Wall Temperatures

Because the variations in longitudinal and circumferential temperature profiles of the inside-wall temperature were consistent, circumferential average temperatures are used in the following comparisons.

Exhaust-gas temperature. - The variations in the longitudinal profile of the average inside-wall temperature with exhaust-gas temperature level is shown in figure 16. The inside-wall temperature increases from the flame holder to the exhaust-nozzle inlet with exhaust-gas temperature level. The variation of wall temperature with exhaust-gas temperature level is slight at stations C and D because the flame has not spread to the wall. The wall temperatures at these stations are influenced more by the mass flow and inlet temperature of the cooling air than by the exhaust-gas temperature level. Downstream of station D, the wall temperature

increases because the temperature gradients near the wall and the radiant heat transfer increase as exhaust-gas temperature level increases. The profiles shown were obtained with a mass-flow ratio of approximately 0.145. The effect of mass-flow ratio on the wall temperature will be shown in the Combustion-Gas Mass Flow section.

Fuel distribution. - The effect of fuel distribution on the inside-wall temperatures is shown in figure 17 for an average exhaust-gas temperature of 3290° R and a mass-flow ratio of 0.145. The curves have been extrapolated linearly to station G, as indicated by the data of figures 16 and 18, because only two thermocouples were functioning during these readings and the temperatures at these positions were usually higher than the circumferential average temperature. Configuration B had the highest average inside-wall temperature as a result of the very high gas temperatures at the bottom of the burner; the average inside-wall temperatures of configuration A are intermediate, whereas configuration C had the lowest wall temperatures as a result of the lower gas-temperature gradients near the walls of the burner. For the two extremes in fuel distribution tested, the spread in average inside-wall temperatures at station F was 235° F, but the circumferential variations in wall temperature were greatest with configuration B.

Combustion-gas mass flow. - With an average mass-flow ratio of 0.144, the average inside-wall temperature was lowered 40° to 100° at stations F and G when the mass flow of combustion gas was decreased from 22.29 to 13.85 pounds per second (fig. 18). Comparison of the wall temperatures at the lower mass flow with wall temperatures interpolated from figure 16 indicates, however, that these reductions resulted primarily from the decrease in exhaust-gas temperature level.

Effect of Mass-Flow Ratio and Cooling-Air Temperature on

Average Inside-Wall Temperatures

Mass-flow ratio. - The effect of cooling-air mass-flow ratio on the average inside-wall temperature is shown in figure 19. The limiting values of the average inside-wall temperature at stations C, D, and E with no cooling-air flow were assumed to coincide with their respective average gas temperatures 1/4 inch from the inside wall with no cooling-air flow.

As previously discussed, the inside-wall temperatures at stations C and D are nearly independent of the exhaust-gas temperature level and vary inversely with mass-flow ratio. The higher wall temperatures at station D result from increased radiant heat transfer from the combustion zone. Both radiant and convective heat transfer became important downstream of station D as a result of the higher gas-temperature level and

the flame impingement on the walls. Thus, from station D on downstream, a distinct curve results for each tail-pipe fuel-air ratio (exhaust-gas temperature level) as shown in figure 19. Figure 19(a) shows that no cooling air is required in the first 24 inches downstream of the flame holder (station D) if the tail-pipe materials can withstand nonafter-burning operation without cooling.

A mass-flow ratio of 0.12 is required in order to maintain an average inside-wall temperature of 1300° F, 48 inches downstream of the flame holder (station F) with an exhaust-gas temperature of 3825° R, and the mass-flow ratio is about 0.09 with an exhaust-gas temperature of 3435° R. An average inside-wall temperature of 1300° F, 56 inches downstream of the flame holder (station G), requires a mass-flow ratio of approximately 0.115 at 3435° R. An average inside-wall temperature of 1300° F was selected as representative in order to allow for possible hot spots as high as 1600° F.

Cooling-air temperatures. - The variation of inside-wall temperature with inlet cooling-air temperature (fig. 20) is similar for all exhaust-gas temperatures but differs in temperature level. The wall temperature increased with a slightly increasing rate as the cooling-air temperature was increased. When the inlet cooling-air temperature was increased 1000° F, the inside-wall temperatures increased at stations F and G about 400° F at a mass-flow ratio of 0.145. The inside-wall temperatures at station G (fig. 20(b)) were about 100° F higher than at station F (fig. 20(a)) with an exhaust-gas temperature of approximately 3060° R, and about 150° higher with an exhaust-gas temperature of 3435° R.

Interrelation of Temperatures

The interrelation of the exhaust-gas temperature, gas temperatures near the wall, inside-wall temperature, and cooling-air temperatures are shown in figure 21 for station F. The cooling-air temperature rise to station F is the vertical distance between the cooling-air temperature curve and the diagonal dashed line. This rise in cooling-air temperature becomes small as the inlet cooling air is raised to temperatures of 1500° to 1700° R, indicating that a combustion chamber with an inner liner maintains a layer of gas at approximately turbine-outlet temperature next to the outside structural wall. Consequently, the temperature of the structural wall of an insulated tail-pipe burner having an inner liner would be practically the same with or without tail-pipe burning.

The data of figure 22 can be shown to better advantage by means of the parameter $\frac{T_{g,F} - T_{w,F}}{T_{w,F} - T_{a,F}}$ which is obtained from a heat balance across the inside wall at station F. This parameter is the ratio of the over-

all heat-transfer coefficients on the cooling-air and combustion-gas sides of the inside wall H_a/H_g . The ratio H_a/H_g is a function of the inlet cooling-air temperature, exhaust-gas temperature, turbine-discharge gas temperature, and mass-flow ratio for a given fuel distribution and burner geometry. This parameter can be plotted against the ratio of the inlet cooling-air temperature to the exhaust-gas temperature $T_{a,B}/T_g$ for given mass-flow ratios, turbine-discharge gas temperatures, and radial fuel distributions. Inasmuch as the cooling-air temperature $T_{a,F}$ and the effective-gas temperature $T_{g,F}$ are not generally known, and because these temperatures are functions of the same variable as the ratio H_a/H_g , the more convenient parameter $\frac{T_g - T_{w,F}}{T_{w,F} - T_{a,B}}$ is plotted in figure 22 against $\frac{T_{a,B}}{T_g}$. The parameter $\frac{T_g - T_{w,F}}{T_{w,F} - T_{a,B}}$ varies approximately linearly with $\frac{T_{a,B}}{T_g}$ but varies in level and slope with the radial fuel distribution and mass-flow ratio. The upper curve is for configuration C with a mass-flow ratio of 0.143. The second curve from the top is the mean line through the data of configuration A with mass flows of combustion gas of 22.3 and 13.8 pounds per second at a mass-flow ratio of approximately 0.143. The effect of exhaust-gas temperature level from 3064° to 3845° R is not apparent within the scatter of the data. The large discrepancy between the data points and the curve for configuration A at $\frac{T_{a,B}}{T_g} = 0.54$ amounts to only 41° R in $T_{w,F}$. The parameter $\frac{T_g - T_{w,F}}{T_{w,F} - T_{a,B}}$ is very sensitive to small changes in $T_{w,F}$ for values of $\frac{T_{a,B}}{T_g}$ greater than approximately 0.50.

The third curve is for configuration A at a mass-flow ratio of 0.098. The data of configuration C fall along the lowest curve at a mass-flow ratio of 0.143.

COOLING-AIR PRESSURE DROP

The pressure drop through the cooling passage is shown in figure 23 against the cooling-air flow. The use of σ based on inlet temperature and pressure satisfactorily correlated the data. The pressure drop increases with exhaust-gas temperature because of increased momentum pressure drop accompanying higher heat transfer to the cooling air.

The isothermal friction factor for the instrumented cooling passages is shown in figure 24. The turbulence created by the instrumentation and the interlocking stringers was great enough to make the friction factor practically independent of Reynolds number. The value was about 0.009 for a Reynolds number range of 1.6×10^4 to 1.3×10^5 . Without the instrumentation the friction factor should lie closer to the line for commercial pipe.

SUMMARY OF RESULTS

The effects of tail-pipe fuel-air ratio (exhaust-gas temperature level), radial distribution of tail-pipe fuel, and mass flow of combustion gas on the temperature profiles of the combustion gas and inside wall of the combustion chamber were determined for an experimental tail-pipe burner cooled by air flowing through an insulated cooling-air passage 1/2 inch in height.

Large circumferential variations existed in the combustion-gas temperature near the inside wall. These variations in combustion-gas temperature resulted in similar variations in the inside-wall temperature. The difference between the highest and the lowest gas temperatures around the circumference 1/4 inch from the inside wall was approximately 500° to 900° F, whereas the corresponding difference in the inside-wall temperatures was 400° to 600° F. These circumferential variations formed consistent patterns that were similar, although different in magnitude, for all configurations tested.

The two extremes in radial distribution of tail-pipe fuel flow, high fuel concentration toward the combustion-chamber wall and high fuel concentration in the center of the combustion chamber, produced a spread in circumferential average inside-wall temperatures of 235° F at a station 48 inches downstream of the flame holder. The configuration having a high fuel concentration toward the wall presented more of a cooling problem than is indicated by the difference in average inside-wall temperatures because the circumferential variation in temperature was greatest for this configuration.

The distance downstream of flame holders at which the flame spread to the inside wall, as determined from measurements of combustion-gas temperature near the wall, was practically unaffected by tail-pipe fuel-air ratio. However, the spread of the flame toward the wall was a function of radial fuel distribution. At no time did the flame impinge on the inside wall closer than 24 inches downstream of the flame holder. Radiant heat transfer to this section of the inside wall was insufficient as to require wall cooling in the first 24 inches if the tail-pipe materials could withstand nonafterburning operation without cooling.

With the most uniform distribution of tail-pipe fuel tested and an inlet cooling-air temperature of 520° R, an average inside-wall temperature of 1300° F at a station 48 inches downstream of the flame holder required mass-flow ratios of 0.12 and 0.09 at exhaust-gas temperatures of 3825° and 3435° R, respectively. Increasing the distance to 56 inches downstream of the flame holder necessitated a mass-flow ratio of 0.115 with an exhaust-gas temperature of 3435° R.

At a mass-flow ratio of 0.145, the inside-wall temperatures at a station 48 inches downstream of the flame holder were increased approximately $4/10^{\circ}$ per degree increase in inlet cooling-air temperature.

It was shown that the temperature of the structural wall of an insulated tail-pipe burner having an inner liner would be practically the same with or without tail-pipe burning.

Lewis Flight Propulsion Laboratory
National Advisory Committee for Aeronautics
Cleveland, Ohio.

APPENDIX A

CALCULATION OF EXHAUST-GAS TEMPERATURE

The exhaust-gas temperature was calculated from the following equation when the nozzle was choked:

$$T_g = \gamma_g \frac{(\gamma_g + 1)}{2} \frac{g}{R} \left(\frac{p_n C_n C_T A_n}{W_g} \right)^2 \quad (B1)$$

where $C_n = 0.965$.

$$C_T = [1 + 9 \times 10^{-6} (t_n - 70)]^2$$

and p_n was obtained from the critical pressure ratio corresponding to γ_g

$$p_n = P_n \left(\frac{\gamma_g + 1}{2} \right)^{\frac{\gamma_g}{\gamma_g - 1}}$$

When the nozzle was unchoked

$$T_g = \frac{(\gamma_g - 1)}{\gamma_g} \frac{g}{W_g^2} \frac{1}{2R} \frac{1}{\left[1 - \left(\frac{p_0}{p_n} \right)^{\frac{\gamma_g - 1}{\gamma_g}} \right]} \left(\frac{F_j}{C_j} \right) \quad (B2)$$

where $C_j = 0.97$.

2408

APPENDIX B

SYMBOLS

A_n	area of exhaust-nozzle throat at 70° F, sq ft
C_j	ratio of scale jet thrust to ideal jet thrust
C_n	exhaust-nozzle flow coefficient
C_T	area thermal expansion coefficient
D_h	hydraulic diameter of cooling passage (twice cooling passage height), ft
F_j	scale jet thrust, lb
f	isothermal friction factor
f/a	fuel-air ratio
$(f/a)_t$	tail-pipe fuel-air ratio
g	acceleration due to gravity, ft/sec ²
H_a	combined coefficient of heat transfer on the cooling-air side, Btu/(hr)(sq ft)(°R)
H_g	combined coefficient of heat transfer on combustion-gas side, Btu/(hr)(sq ft)(°R)
l	flow distance between stations B and F, ft
P_n	total pressure at exhaust-nozzle throat, lb/sq ft abs.
P_5	turbine-outlet total pressure, lb/sq ft abs.
P_8	exhaust-nozzle total pressure, lb/sq ft abs.
P_0	static pressure in tunnel test section, lb/sq ft abs.
P_n	static pressure at exhaust-nozzle throat, lb/sq ft abs.
\bar{q}	average dynamic pressure between stations B and F, lb/sq ft
R	gas constant, ft-lb/(lb)(°R)
Re	Reynolds number

T_a	cooling-air temperature, $^{\circ}\text{R}$ or $^{\circ}\text{F}$
T_g	exhaust-gas temperature at nozzle exit, $^{\circ}\text{R}$
$T_{g,1/4}$	combustion-gas temperature measured 1/4 inch from inside wall, $^{\circ}\text{R}$ or $^{\circ}\text{F}$
$T_{g,1/2}$	combustion-gas temperature measured 1/2 inch from inside wall, $^{\circ}\text{R}$ or $^{\circ}\text{F}$
T_s	outside-wall temperature, $^{\circ}\text{F}$
T_s'	turbine-outlet total temperature, $^{\circ}\text{R}$
T_w	inside-wall temperature, $^{\circ}\text{R}$ or $^{\circ}\text{F}$
T_1	engine-inlet total temperature, $^{\circ}\text{R}$
t_n	average temperature of exhaust nozzle lip, $^{\circ}\text{F}$
W_a	cooling-air flow, lb/sec
$W_{f,e}$	engine fuel flow, lb/hr
$W_{f,t}$	tail-pipe fuel flow, lb/hr
W_g	combustion gas flow, lb/sec
W_a/W_g	mass-flow ratio
γ_g	ratio of specific heats of exhaust gas corresponding to total fuel-air ratio and exhaust-gas temperature
$\eta_{b,t}$	tail-pipe combustion efficiency
σ	ratio of density at prevailing temperature and pressure to density at standard temperature and pressure

Subscripts:

B to G longitudinal stations

REFERENCES

1. Koffel, William K., Stamper, Eugene, and Sanders, Newell D.: Cooling of Ram Jets and Tail-Pipe Burners - Analytical Method for Determining Temperatures of Combustion Chamber Having Annular Cooling Passage. NACA RM E9L09, 1950.

2. Conrad, E. William, and Jansen, Emmert T.: Effects of Internal Configurations on Afterburner Shell Temperatures. NACA RM E51I07
3. Wallner, Lewis E., and Jansen, Emmert T.: Full-Scale Investigation of Cooling Shroud and Ejector Nozzle for a Turbojet Engine - Afterburner Installation. NACA RM E51J04
4. Sibulkin, Merwin, and Koffel, William K.: Chart for Simplifying Calculations of Pressure Drop of a High-Speed Compressible Fluid under Simultaneous Action of Friction and Heat Transfer - Application to Combustion-Chamber Cooling Passages. NACA TN 2067, 1950.
5. Flock, Ernest F., and Dahl, Andrew I.: Sixteenth Monthly Report of Progress on the Development of Thermocouple Pyrometers for Gas Turbines. Nat. Bur. Standards. April 14, 1947.
6. Blackshear, Perry L., Jr.: Sonic-Flow-Orifice Temperature Probe for High-Gas-Temperature Measurements. NACA TN 2167, 1950.



TABLE I. - OPERATING CONDITIONS

Run	Altitude (ft)	Exhaust nozzle exit area (sq ft)	Flight Mach number M_0	Ambient pressure P_0 (lb/sq ft abs.)	Engine-inlet total pressure P_2 (lb/sq ft abs.)	Engine-inlet total temperature T_1 (°R)	Cooling-air inlet temperature T_a (°R)	Engine fuel flow $W_{f,t}$ (lb/hr)	Tail pipe fuel flow $W_{f,t}$ (lb/hr)	Engine air flow W_a (lb/sec)	Total fuel-air ratio $(\frac{f}{a})$	Tail pipe fuel-air ratio $(\frac{f}{a})_t$	Mass ratio $\frac{W_a}{W_g}$	Tail-pipe combustion efficiency $\eta_{b,b}$	Turbine-outlet total pressure P_5 (lb/sq ft abs.)	Turbine-outlet total temperature T_5 (°R)	Exhaust-nozzle total pressure P_8 (lb/sq ft abs.)	Exhaust-gas total temperature T_g (°R)	Run	
CONFIGURATION A																				
1	50,000	1.846	0.512	833	757	506	541	1194	1885	21.05	0.0407	0.0525	0.0672	0.959	1373	1640	1272	2894	1	
2			.520	888	755	508	550	1186	1845	21.14	.0588	.0515	.0614	.871	1350	1632	1248	2858	2	
3			.521	827	753	484	526	1268	2090	21.95	.0425	.0545	.1005	.885	1432	1630	1527	2983	3	
4			.549	820	761	501	518	1204	1855	21.40	.0587	.0513	.1028	.902	1361	1627	1271	2891	4	
5			.518	827	751	508	522	1194	1850	20.85	.0518	.0523	.1033	.945	1361	1645	1261	2895	5	
6			.522	826	753	508	518	1190	1850	21.06	.0574	.0518	.1218	.919	1365	1637	1261	2954	6	
7			.511	830	753	497	518	1263	2050	21.18	.0432	.0547	.0968	.945	1415	1636	1513	3117	7	
8			.521	827	754	504	536	1235	1890				.0949			1622			8	
9			.514	829	753	503	535	1222	1970	20.89	.0422	.0539	.0960	.965	1397	1621	1296	3106	9	
10			.516	827	753	503	535	1221	1955	21.05	.0419	.0535	.1002	.964	1396	1630	1296	3086	10	
11			.512	829	753	503	542	1230	1855	20.89	.0422	.0536	.0968	.989	1400	1627	1296	3110	11	
12			.519	826	753	503	548	1225	1955	21.06	.0419	.0535	.0965	.959	1396	1622	1296	3081	12	
13			.511	828	748	497	525	1259	2005	21.15	.0426	.0544	.0948	.955	1408	1632	1507	3110	13	
14			.510	828	750	508	1037	1225	1855	20.88	.0423	.0539	.0960	.967	1385	1629	1285	3121	14	
15			.507	831	752	508	1115	1228	1850	20.86	.0423	.0538	.0988	.978	1385	1635	1285	3123	15	
16			.512	829	753	507	1245	1251	1850	21.05	.0420	.0535	.0964	.944	1393	1630	1292	3063	16	
17			.510	829	751	508	1343	1232	1855	21.11	.0417	.0532	.0985	.942	1392	1632	1291	3045	17	
18			.508	832	753	508	1415	1211	1850	20.95	.0416	.0532	.1016	.976	1392	1622	1291	3084	18	
19			.524	828	757	499	494	909	0	22.92	.0310	.0310	.0989		969	1185	866		19	
20			.518	829	756	505	500	907	0	21.25	.0319	.0318	.0987		969	1188	868		20	
21			.515	831	756	503	508	960	1485	21.66	.0516	.0288	.1012	.504	1156	1350	1043	1706	21	
22			.514	833	758	504	510	1075	1615	21.48	.0574	.0290	.1005	.645	1259	1451	1162	2589	22	
23			.511	831	754	506	625	1151	1975	21.41	.0406	.0328	.1041	.756	1358	1561	1255	2702	23	
24			.509	831	752	508	625	1170	2015	21.28	.0416	.0336	.1029	.779	1348	1570	1244	2787	24	
25			.508	831	753	514	555	1255	2019	20.94	.0433	.0330	.0662	.958	1392	1641	1291	3121	25	
26			.514	828	753	503	546	1244	2032	21.15	.0431	.0347	.0694	.924	1404	1632	1302	3088	26	
27			.518	828	753	503	529	1248	1988	21.15	.0427	.0341	.0985	.948	1410	1624	1306	3102	27	
28			.519	827	753	499	529	1284	2085	21.48	.0434	.0352	.1208	.900	1421	1638	1517	3059	28	
29			.508	831	753	503	517	1268	2079	21.15	.0440	.0356	.1519	.841	1422	1636	1517	3152	29	
30			.508	839	751	503	507	1268	2079	21.35	.0438	.0352	.1872	.822	1428	1632	1525	3102	30	
31			.514	831	755	520	541	1221	1998	20.78	.0429	.0348	.1467	.816	1390	1648	1278	3078	31	
32			.514	831	755	511	857	1200	1998	21.05	.0422	.0344	.1482	.903	1400	1634	1298	3101	32	
33			.518	829	755	504	750	1183	2028	21.24	.0420	.0345	.1255	.945	1408	1632	1505	3063	33	
34			.518	829	754	508	850	1158	2045	21.08	.0424	.0351	.1447	.957	1407	1637	1505	3104	34	
35			.520	828	756	503	1028	1224	1996	21.50	.0418	.0377	.1428	.948	1412	1626	1510	3067	35	
36			.528	827	755	505	1153	1221	1996	21.39	.0417	.0359	.1458	.938	1412	1624	1510	3040	36	
37			.511	836	760	501	1355	1220	1988	21.54	.0414	.0353	.1410	.945	1421	1630	1517	3028	37	
38			.520	830	757	506	1462	1228	1978	21.34	.0417	.0354	.1391	.958	1415	1628	1513	3068	38	
39			.521	831	759	508	1687	1230	1978	21.42	.0416	.0353	.1417	.958	1415	1638	1512	3040	39	
40			.518	828	754	506	908	869	0	21.17	.0317	.0317	.1040		958	1206	890		40	
41			.513	827	751	500	1556	819	1615	21.37	.0516	.0285	.1455	.578	1165	1568	1064	1806	41	
42			.518	827	752	503	1590	974	2005	21.27	.0509	.0332	.1413	.636	1359	1548	1257	2752	42	
43			.514	831	753	508	1850	1217	1942	21.16	.0415	.0331	.1459	.960	1404	1631	1502	3067	43	
44	50,000	1.905	0.518	828	755	504	519	1262	2360	21.28	0.0473	0.0401	0.1216	0.888		1654	1503	1525	3215	44
45			.488	834	751	508	513	1262	2360	20.94	.0480	.0409	.1444	.827		1640	1504	1525	3233	45
46			.510	828	751	508	513	1285	2255	20.94	.0467	.0382	.1688			1649				46
47			.511	830	753	508	515	1285	2280	21.05	.0468	.0381	.1917	.936		1647	1598	1525	3282	47
48			.509	828	748	508	514	1248	2227	20.77	.0463	.0387	.1481	.981	1405	1627	1298	3541	48	

49	50,000	1.905	0.512	651	756	501	788	1243	2217	21.34	0.0480	0.0574	0.1420	0.928	1408	1617	1296	3175	49
50			.530	625	751	499	859	1253	2259	21.32	.0465	.0579	.1398	.823	1408	1622	1298	3188	50
51			.515	627	751	501	815	1243	2166	21.22	.0469	.0572	.1441	.948	1406	1624	1296	3207	51
52			.514	628	752	505	1013	1224	2186	21.12	.0448	.0574	.1445	.970	1408	1622	1297	3237	52
53			.518	629	754	503	1117	1221	2186	21.23	.0446	.0571	.1427	.967	1405	1615	1295	3204	53
54			.521	627	754	506	1222	1235	2186	21.15	.0450	.0375	.1424	.850	1400	1616	1395	3214	54
55			.518	630	756	506	500	890	0	22.54	.0117	.0117	.1039	-----	961	1188	878	-----	55
56			.520	628	756	506	509	938	1290	22.49	.0291	.0198	.1048	.094	1068	1280	857	1352	56
57			-----	630	-----	499	500	1002	1595	-----	-----	-----	-----	-----	1184	1347	1085	-----	57
58			.509	631	753	504	809	1068	1840	22.45	.0382	.0299	.1026	.490	1249	1451	1139	2160	58
59			-----	629	-----	510	512	1048	1770	-----	-----	-----	-----	-----	1221	1448	1111	-----	59
60			.505	633	753	505	515	1142	1865	22.47	.0396	.0310	.1025	.816	1321	1538	1215	2904	60
61			.521	632	760	505	500	1171	2060	22.47	.0417	.0354	.1002	.829	1327	1525	1254	2922	61
62	30,000	1.980	0.511	632	755	507	833	1238	2620	20.87	0.0515	0.0463	0.0935	0.953	1400	1630	1290	3216	62
63			.509	631	753	506	830	1247	2680	21.00	.0517	.0459	.1080	.830	1405	1640	1294	3434	63
64			.518	631	787	504	828	1247	2615	21.24	.0505	.0444	.1071	.858	1410	1627	1299	3443	64
65			.518	628	754	505	828	1250	2610	21.17	.0508	.0446	.1326	.945	1411	1638	1500	3470	65
66			-----	629	-----	510	820	1220	2590	-----	-----	-----	-----	-----	1388	1629	-----	-----	66
67			.520	629	758	497	518	1250	2620	21.58	.0505	.0443	.1524	.851	1414	1625	1505	3422	67
68			-----	628	-----	512	1241	2545	-----	-----	-----	-----	-----	-----	1395	1636	1282	-----	68
69			.520	628	756	505	823	1260	2600	21.50	.0508	.0441	.1689	.925	1409	1625	1297	3408	69
70			.524	629	758	505	902	1259	2590	21.45	.0499	.0438	.1796	.829	1415	1620	1308	3401	70
71			.512	632	758	512	1046	1227	2600	20.87	.0509	.0451	.1571	.832	1396	1637	1285	3457	71
72			.521	627	754	513	1059	1212	2610	20.88	.0509	.0435	.1711	.918	1391	1646	1278	3427	72
73			.516	629	754	504	1050	1240	2620	21.22	.0506	.0447	.1715	.910	1410	1637	1285	3594	73
74			.522	624	751	498	495	889	0	21.41	.0315	.0118	.0992	-----	964	1182	850	-----	74
75			.519	628	754	506	511	915	1585	21.15	.0504	.0215	.0974	.102	1040	1241	833	1353	75
76			.518	629	755	509	580	1220	21.00	.0325	.0239	.1010	.275	1094	1308	887	1659	76	
77			.512	627	750	500	502	967	1845	21.27	.0344	.0268	.1000	.388	1147	1342	1041	1690	77
78			.511	631	754	500	507	1078	2000	21.50	.0401	.0323	.0966	.793	1280	1455	1150	2737	78
79			.512	632	756	505	512	1163	2150	21.50	.0452	.0358	.1008	.835	1335	1585	1226	3108	79
80			.524	628	759	507	830	1240	2710	21.10	.0520	.0465	.1000	.908	1405	1638	1294	3449	80
81			.521	625	752	505	620	1233	2592	21.25	.0501	.0441	.1436	.925	1401	1628	1289	3594	81
82			.507	620	751	505	669	1223	2600	20.96	.0507	.0443	.1480	.852	1401	1631	1289	3481	82
83			.518	624	749	507	771	1213	2612	20.98	.0507	.0450	.1411	.821	1394	1632	1285	3425	83
84			-----	629	-----	512	888	1261	2644	-----	-----	-----	-----	-----	1400	1637	1285	-----	84
85			.512	626	749	504	1049	1236	2628	21.02	.0510	.0452	.1578	.851	1408	1631	1289	3454	85
86			.522	624	751	505	1135	1228	2621	21.17	.0506	.0446	.1428	.912	1398	1627	1296	3593	86
87			-----	625	-----	512	1229	1588	2628	-----	-----	-----	-----	-----	1398	1632	1287	-----	87
88			.511	631	756	506	1309	1402	2628	21.18	.0528	.0449	.1430	.909	1408	1631	1291	3402	88
89			.510	629	751	498	1408	1251	2512	21.26	.0505	.0444	.1412	.919	1409	1625	1296	3405	89
90	40,000	1.980	0.515	392	471	805	848	828	1411	13.16	0.0473	0.0585	0.1415	0.821	853	1281	782	3272	90
91			.522	392	473	804	828	804	1341	13.25	.0459	.0586	.1451	.879	859	1280	791	3284	91
92			.525	393	473	805	720	822	1264	13.25	.0434	.0543	.1440	1.028	854	1207	786	3282	92
93			.522	392	472	805	837	831	1289	13.26	.0438	.0544	.1415	1.013	858	1212	786	3258	93
94			.525	393	470	501	1013	820	1292	13.16	.0448	.0535	.1438	.970	848	1208	778	3225	94
95			.524	394	471	506	1154	817	1308	13.05	.0453	.0531	.1458	.963	848	1215	778	3281	95
96			.529	389	469	500	1210	851	1275	13.23	.0442	.0547	.1366	.994	854	1211	785	3244	96
97			.522	392	469	504	1340	829	1306	12.89	.0457	.0563	.1418	.986	847	1217	779	3306	97
98	50,000	2.12	0.514	636	761	501	523	1288	2665	21.57	0.0681	0.0650	0.1574	0.825	1427	1637	1302	3211	98
99			.518	634	760	504	520	1273	2670	21.47	.0686	.0653	.1651	.820	1427	1642	1299	3217	99
100			.515	631	758	506	515	1268	2670	21.24	.0670	.0680	.1671	.823	1415	1642	1291	3245	100
101			.518	634	761	503	508	1087	2296	21.62	.0437	.0567	.1906	-----	1269	1458	1147	-----	101
102			.511	630	753	500	510	1177	2250	21.44	.0322	.0470	.1884	.824	1340	1522	1218	2490	102

^aBased on average V_g .

^bApproximately 0.615.

NACA

TABLE I. - OPERATING CONDITIONS - Concluded

Run	Altitude (ft)	Exhaust nozzle exit area (sq ft)	Flight Mach number M_0	Ambient pressure P_0 ($\frac{\text{lb}}{\text{sq ft abs.}}$)	Engine-inlet total pressure P_2 ($\frac{\text{lb}}{\text{sq ft abs.}}$)	Engine-inlet total temperature T_1 ($^{\circ}\text{R}$)	Cooling-air inlet temperature T_a ($^{\circ}\text{R}$)	Engine fuel flow $W_{f,e}$ ($\frac{\text{lb}}{\text{hr}}$)	Tail-pipe fuel flow $W_{f,t}$ ($\frac{\text{lb}}{\text{hr}}$)	Engine air flow W_a ($\frac{\text{lb}}{\text{sec}}$)	Total fuel-air ratio ($\frac{\text{lb}}{\text{lb}}$)	Tail-pipe fuel-air ratio ($\frac{\text{lb}}{\text{lb}}$)	Mass ratio $\frac{W_a}{W_g}$	Tail-pipe combustion efficiency $\eta_{b,t}$	Turbine-outlet total pressure P_5 ($\frac{\text{lb}}{\text{sq ft abs.}}$)	Turbine-outlet total temperature T_5 ($^{\circ}\text{R}$)	Exhaust-nozzle total pressure P_8 ($\frac{\text{lb}}{\text{sq ft abs.}}$)	Exhaust-gas total temperature T_8 ($^{\circ}\text{R}$)	Run
CONFIGURATION B																			
1	50,000	1.903	0.511	830	753	508	507	1255	2359	21.14	0.0475	0.0402	0.0985	0.804	1408	1818	1300	3248	1
2			.524	825	754	501	507	1260	2355	21.45	.0468	.0398	.1198	.873	1409	1823	1301	3181	2
3			.519	827	753	507	500	1282	2345	21.22	.0478	.0398	.1422	.865	1410	1831	1298	3215	3
4			.514	829	753	504	500	1279	2373	21.28	.0477	.0405	.1891	.890	1414	1836	1305	3232	4
5			.516	828	753	501	500	1258	2365	21.42	.0469	.0397	.1891	.860	1404	1822	1298	3140	5
6			.514	828	752	504	495	1268	2375	21.01	.0481	.0409	.1449	.921	1416	1833	1308	3305	6
7			.524	828	757	505	748	1236	2342	21.29	.0487	.0397	.1417	.894	1411	1828	1301	3187	7
8			.511	831	754	503	737	1243	2345	21.17	.0471	.0400	.1452	.937	1422	1838	1311	3289	8
9			.514	829	753	504	838	1251	2345	21.04	.0475	.0392	.1460	-----	1421	1833	-----	-----	9
10			.512	829	752	507	938	1250	2337	20.94	.0476	.0403	.1457	.921	1408	1830	1299	3285	10
11			.525	828	759	506	1058	1158	2425	21.42	.0464	.0408	.1412	.878	1408	1823	1299	3156	11
12			.514	830	754	507	1127	1129	2438	21.08	.0470	.0418	.1425	.893	1398	1817	1289	3206	12
13			.512	828	751	501	1223	1115	2459	21.22	.0468	.0418	.1425	.875	1399	1822	1289	3164	13
CONFIGURATION C																			
1	50,000	1.903	0.512	832	758	505	524	1251	2190	21.28	0.0450	0.0372	0.1478	0.872	1412	1825	1306	3248	1
2			.507	834	756	500	725	1258	2210	21.43	.0450	.0370	.1419	.957	1420	1827	1312	3280	2
3			.515	827	751	496	828	1259	2195	21.39	.0448	.0372	.1428	.955	1415	1824	1308	3214	3
4			.510	829	751	501	925	1257	2188	21.28	.0451	.0370	.1438	.963	1412	1825	1307	3237	4
5			.504	824	754	498	1040	1244	2190	21.34	.0447	.0372	.1399	.990	1419	1822	1313	3252	5
6			.512	832	758	505	1233	1386	2190	21.33	.0486	.0371	.1416	.875	1417	1831	1312	3245	6
7			.510	833	756	500	1450	1424	2160	21.36	.0469	.0373	.1413	.890	1417	1828	1312	3237	7
8	50,000	2.18	0.510	834	757	508	524	1205	4365	20.84	0.0743	0.0752	0.1912	0.716	1389	1611	1286	3784	8

NACA

TABLE II - CIRCUMFERENTIAL AVERAGE TEMPERATURES, °F



Run	Station C				Station D				Station E				Station F				Run					
	Combustion gas		Inside wall	Outside wall	Cooling air	Combustion gas		Inside wall	Outside wall	Cooling air	Combustion gas		Inside wall	Outside wall	Cooling air	Combustion gas		Inside wall	Outside wall	Cooling air		
	T _{G,1/2}	T _{G,1/4}	T _w	T _s	T _a	T _{G,1/2}	T _{G,1/4}	T _w	T _s	T _a	T _{G,1/2}	T _{G,1/4}	T _w	T _s	T _a	T _{G,1/2}		T _{G,1/4}	T _w	T _s	T _a	
COMBUSTION A																						
1	1098	1085	711	125	110	1517	1127	843	229	204	1887	1410	983	525	391	1819	1835	1198	489	595	1	
2	1085	1085	661	100	93	1290	1110	780	185	174	1550	1588	884	258	243	1818	1828	1107	405	350	2	
3	1100	1087	800	78	84	1542	1148	708	157	148	1896	1449	822	198	207	2113	1858	1080	508	268	3	
4	1082	1079	800	75	73	1273	1107	706	153	144	1517	1359	799	195	201	1784	1878	948	508	269	4	
5	1091	1098	612	82	81	1505	1105	728	150	153	1561	1597	838	214	215	1815	1889	1046	539	290	5	
6	1085	1090	864	73	75	1292	1090	683	124	159	1525	1587	759	178	188	1805	1807	982	281	282	6	
7	1103	1078	631	72	70	1510	1114	889	188	141	1684	1458	817	188	186	2007	1756	1059	515	389	7	
8	1095	1074	868	100	92	1286	1111	749	173	170	1611	1445	892	255	227	1951	1787	1032	589	548	8	
9	1098	1078	891	202	181	1299	1180	788	285	252	1652	1448	912	356	312	1968	1774	1038	502	415	9	
10	1105	1079	775	392	388	1298	1125	854	458	441	1645	1456	866	494	448	1956	1777	1080	610	568	10	
11	1089	1089	888	489	492	1298	1119	884	580	538	1873	1480	1015	575	572	1979	1795	1157	686	638	11	
12	1087	1078	858	498	500	1505	1151	888	827	844	1849	1480	1011	577	581	1972	1805	1154	686	844	12	
13	1102	1082	851	508	514	1282	1109	882	856	554	1888	1458	1011	681	688	1981	1778	1143	680	650	13	
14	1119	1100	885	582	583	1324	1189	916	591	808	1681	1499	1044	638	640	1987	1884	1188	785	701	14	
15	1150	1110	915	681	682	1311	1198	983	668	845	1702	1511	1086	707	720	2011	1855	1201	781	771	15	
16	1154	1118	983	775	788	1548	1186	1032	782	812	1727	1558	1147	820	829	2022	1856	1256	889	876	16	
17	1137	1146	1042	872	887	1527	1217	1090	869	910	1778	1511	1205	907	918	2043	1877	1302	977	968	17	
18	1150	1158	1075	989	956	1514	1210	1122	932	972	1728	1532	1228	968	978	1987	1889	1364	1028	1012	18	
19	721	687	588	37	38	-----	-----	363	54	74	-----	-----	398	71	101	-----	-----	565	83	112	19	
20	704	651	548	44	45	-----	-----	368	81	80	-----	-----	370	85	104	-----	-----	571	112	128	20	
21	847	817	468	50	52	-----	-----	460	77	88	1051	-----	469	103	154	1105	1085	514	145	156	21	
22	858	980	469	58	82	-----	-----	541	97	114	1216	-----	573	151	180	1504	1288	661	168	181	22	
23	1046	1025	521	73	77	1127	1061	623	124	159	1355	1145	681	173	198	1658	1445	789	250	245	23	
24	1083	1048	534	71	76	1149	1041	847	120	153	1404	1185	701	168	188	1775	1533	830	244	247	24	
25	1129	1092	792	151	183	1324	1158	889	262	227	1657	1456	1087	537	510	2111	1865	1226	655	458	25	
26	1065	1085	772	114	118	1518	1138	863	214	207	1850	1411	1088	510	288	2036	1841	1188	473	578	26	
27	1094	1077	884	90	92	1508	1122	774	165	175	1612	1586	918	846	239	1882	1785	1048	378	329	27	
28	1110	1091	843	88	88	1329	1158	731	156	158	1694	1456	878	207	214	1982	1848	1023	355	296	28	
29	1084	1079	882	71	73	1328	1128	667	114	155	1677	1445	788	157	180	2014	1820	812	286	253	29	
30	1077	1062	520	57	61	1299	1119	888	88	118	1835	1548	697	128	159	1985	1770	857	224	206	30	
31	1144	1150	807	123	102	1585	1170	701	198	172	1682	1509	854	248	244	1882	1808	967	370	515	31	
32	1101	1080	840	215	210	1315	1125	897	256	269	1619	1597	846	295	512	1958	1781	966	592	578	32	
33	1103	1082	681	296	306	1508	1156	758	339	358	1624	1411	868	380	396	1853	1781	999	467	454	33	
34	1096	1090	751	378	399	1511	1110	805	415	442	1655	1451	821	458	472	2000	1817	1084	551	523	34	
35	1079	1064	850	684	573	1286	1105	896	579	610	1841	1580	1001	616	635	1985	1801	1158	678	676	35	
36	1102	1078	908	682	674	1305	1120	948	684	705	1885	1594	1054	704	725	2035	1807	1188	757	768	36	
37	1110	1077	1024	842	871	1510	1159	1063	848	892	1639	1420	1159	874	886	2071	1853	1253	820	920	37	
38	1160	1111	1108	886	1000	1508	1189	1148	979	1017	1894	1480	1241	1003	1017	2099	1884	1327	1045	1041	38	
39	1151	1107	1188	1106	1158	1359	1210	1226	1100	1158	1687	1474	1514	1119	1151	2108	1817	1584	1188	1152	39	
40	706	670	547	62	63	-----	-----	582	72	87	-----	-----	586	125	118	-----	-----	580	126	157	40	
41	902	882	912	884	893	-----	-----	913	858	888	-----	-----	1001	922	855	868	1070	1087	923	858	884	41
42	1088	1085	1123	1089	1089	1119	1071	1143	1048	1106	1381	1244	1198	1059	1080	1586	1459	1232	1077	1090	42	
43	1148	1158	1234	1171	1189	1573	1200	1289	1161	1186	1712	1535	1568	1182	1188	2128	1556	1429	1217	1209	43	
44	1100	1087	620	77	78	1502	1088	698	133	165	1727	1479	1478	856	198	208	2255	1968	1032	508	44	
45	1102	1082	683	72	73	1286	1080	658	117	141	1754	1502	808	189	180	2252	1970	922	874	285	45	
46	1106	1061	645	69	70	1505	1065	615	105	132	1711	1528	758	149	177	2102	1909	905	244	239	46	
47	1100	1048	515	86	87	1508	1071	583	95	122	1720	1497	653	135	163	2119	1894	886	211	220	47	
48	1088	1073	584	78	74	1542	1089	687	132	147	1757	1482	618	171	204	2170	1895	945	256	274	48	

49	1083	1071	682	290	882	1524	1080	749	327	341	1710	1475	877	571	585	2138	1858	1028	488	448	48
50	1093	1062	744	384	580	1336	1072	805	408	435	1758	1476	921	451	471	2161	1877	1085	565	585	50
51	1093	1061	794	470	464	1328	1073	844	481	523	1715	1494	978	549	593	2209	1854	1085	827	601	51
52	1099	1069	880	585	563	1323	1084	897	578	812	1728	1474	1020	827	835	2238	1894	1137	703	679	52
53	1100	1073	901	652	662	1328	1085	947	665	897	1728	1477	1065	702	715	2150	1903	1177	779	754	53
54	1113	1091	967	754	765	1349	1110	1009	753	783	1751	1828	1085	797	810	2161	1906	1250	870	846	54
55	690	598	337	52	52	-----	-----	358	77	97	-----	-----	385	105	117	-----	-----	373	151	150	55
56	760	682	385	58	58	-----	-----	420	80	111	-----	-----	340	124	157	-----	-----	486	174	175	56
57	842	738	444	60	63	-----	-----	487	100	122	-----	-----	527	141	153	1184	1053	582	196	202	57
58	837	837	513	70	69	-----	-----	568	119	138	1114	1055	618	173	181	1216	1143	708	246	246	58
59	835	851	501	69	69	-----	-----	534	115	135	1073	1001	617	185	174	1160	1118	685	229	235	59
60	1058	973	590	79	78	1147	-----	670	134	155	1405	1237	752	184	202	1798	1438	817	288	279	60
61	1029	935	580	70	68	1062	-----	640	131	150	1513	1164	735	178	132	1882	1451	685	278	270	61
62	1114	1085	720	108	98	1421	1174	828	189	189	2099	1754	998	292	289	2304	2263	1257	507	593	62
63	1099	1089	895	98	98	1588	1124	783	165	189	1988	1714	988	281	230	2342	2188	1233	451	371	63
64	1085	1101	881	90	88	1420	1174	790	160	173	1850	1867	963	245	240	2487	2148	1187	424	330	64
65	1102	1088	824	81	81	1412	1184	722	133	153	2005	1867	889	197	208	2391	2134	1084	330	301	65
66	1088	1081	580	81	88	1335	1188	838	130	161	1885	1690	658	188	206	2299	2072	1017	307	281	66
67	1104	1083	581	74	73	1381	1144	671	118	141	1988	1630	851	188	191	2289	2084	999	285	271	67
68	1090	1070	544	77	79	1341	1117	598	111	135	1907	1689	788	158	182	2294	2073	957	259	248	68
69	1098	1086	533	69	70	1385	1124	635	108	132	1878	1844	784	152	178	2283	2104	950	260	250	69
70	1096	1080	529	59	60	1330	1139	604	90	118	1824	1593	739	132	161	2290	1978	914	238	228	70
71	1105	1120	688	592	584	1429	1204	822	810	632	2028	1735	1072	654	658	2447	2243	1243	728	716	71
72	1133	1121	870	595	606	1498	1218	828	616	642	2013	1801	1071	658	667	2473	2285	1258	728	719	72
73	1118	1087	654	581	598	1445	1188	904	603	632	2013	1718	1035	639	683	2389	2217	1219	712	700	73
74	716	683	342	58	58	-----	-----	346	57	79	-----	-----	385	79	102	-----	-----	370	107	121	74
75	787	-----	400	62	62	-----	-----	435	91	109	-----	-----	449	120	140	-----	-----	477	160	169	75
76	832	-----	438	89	70	1067	-----	477	102	119	-----	-----	502	135	153	1109	1025	546	188	198	76
77	862	-----	453	82	83	-----	-----	500	86	106	1056	-----	541	118	143	1208	1128	596	169	184	77
78	959	840	827	82	63	1028	-----	595	102	125	1283	1188	672	146	171	1838	1897	781	225	254	78
79	1053	1066	628	77	75	1220	1088	719	129	148	1595	1305	847	189	206	2040	1877	1015	298	288	79
80	1114	1098	701	86	83	1488	1183	821	171	180	2075	1750	1010	271	284	2348	2235	1228	465	402	80
81	1101	1088	695	79	79	1471	1159	882	124	144	1831	1680	883	193	199	2394	2145	1063	307	287	81
82	1099	1108	882	210	218	1508	1178	745	288	280	1818	1698	814	318	329	2409	2174	1108	438	409	82
83	1119	1109	726	535	588	1520	1194	803	389	384	1858	1719	872	430	443	2417	2188	1158	528	518	83
84	1120	1090	776	428	450	1568	1205	841	440	498	2076	1796	1002	480	514	2420	2200	1178	590	572	84
85	1115	1115	860	582	594	1517	1206	813	599	630	2004	1759	1085	843	683	2437	2223	1203	717	708	85
86	1102	1124	818	682	680	1583	1176	877	674	713	2058	1781	1188	719	732	2450	2234	1258	801	783	86
87	1114	1133	975	787	774	1689	1250	1031	785	803	2128	1879	1198	812	819	2486	2263	1348	894	870	87
88	1147	1108	1027	840	851	1508	1178	1077	842	871	2005	1775	1210	885	887	2460	2240	1388	884	935	88
89	1110	1115	1088	851	950	1625	1212	1158	550	984	2019	1771	1281	963	976	2489	2261	1401	1044	1014	89
90	1045	1017	643	181	115	1138	1017	719	289	204	1810	1213	870	568	286	2176	1787	1085	473	389	90
91	1062	1025	618	116	90	1188	1043	704	189	189	1823	1228	878	248	244	2166	1800	1082	353	387	91
92	1089	1013	691	282	378	1154	1024	783	358	339	1578	1228	878	581	387	2094	1740	1087	473	468	92
93	1045	1015	754	409	381	1184	1027	605	458	449	1597	1283	958	508	499	2186	1822	1081	594	586	93
94	1048	1002	845	559	581	1133	1038	882	582	804	1636	1288	1002	624	633	2148	1832	1159	694	681	94
95	1082	1011	928	701	699	1159	1004	972	710	733	1682	1289	1091	744	783	2179	1822	1220	818	804	95
96	1040	1022	953	734	750	1178	1038	994	714	788	1709	1310	1088	741	783	2240	1824	1215	788	787	96
97	1067	1017	1064	884	828	1174	1048	1081	862	931	1680	1283	1181	881	938	2183	1841	1288	931	959	97
98	1083	1068	597	77	78	1737	1179	707	127	145	2810	2330	1018	199	231	2865	2705	1191	384	384	98
99	1080	1081	588	69	75	1748	1167	833	112	133	2817	2300	943	180	201	2840	2877	1121	333	333	99
100	1078	1074	523	67	69	1890	1187	813	100	123	2815	2275	902	131	183	2844	2853	1049	282	257	100
101	947	853	422	51	56	1094	1120	479	77	88	1324	1135	574	89	131	1778	1834	690	188	171	101
102	1031	990	449	57	60	1205	1188	534	88	108	1711	1432	857	120	143	2307	1897	823	214	200	102

NACA

TABLE II - CIRCUMFERENTIAL AVERAGE TEMPERATURES, °F - Concluded

Run	Station C					Station D				Station E				Station F				Run			
	Combustion gas		Inside wall	Outside wall	Cooling air	Combustion gas		Inside wall	Outside wall	Cooling air	Combustion gas		Inside wall	Outside wall	Cooling air	Combustion gas			Inside wall	Outside wall	Cooling air
	T _{g,1/2}	T _{g,1/4}	T _w	T _s	T _a	T _{g,1/2}	T _{g,1/4}	T _w	T _s	T _a	T _{g,1/2}	T _{g,1/4}	T _w	T _s	T _a	T _{g,1/2}	T _{g,1/4}		T _w	T _s	T _a
CONFIGURATION B																					
1	1078	1059	602	72	74	1406	1073	743	123	152	2519	2202	1088	209	264	2758	2599	1254	377	373	1
2	1088	1026	549	60	65	1342	1064	688	99	133	2490	1923	988	181	221	2752	2598	1170	291	313	2
3	1078	1025	510	60	58	1308	1051	627	98	117	2424	2129	900	149	183	2706	2390	1089	221	270	3
4	1069	1031	477	51	56	1182	1082	592	89	109	2512	2009	858	143	189	2585	2404	1067	215	248	4
5	1077	1013	445	52	64	1332	1058	543	81	103	2459	1849	777	110	151	2727	2323	985	169	219	5
6	1083	1044	516	64	67	1382	1078	657	101	130	2600	1936	944	154	207	2718	2410	1164	286	286	6
7	1054	1041	628	290	293	1335	1088	728	321	338	2214	1788	972	361	388	2607	2232	1189	458	468	7
8	1061	1052	635	296	300	1403	1088	737	326	348	2488	1729	989	364	395	2680	2488	1196	463	473	8
9	1073	1087	691	382	388	1427	1111	794	411	431	2307	1797	1062	451	479	2746	2343	1231	543	557	9
10	1099	1031	744	478	465	1437	1128	842	499	521	2415	1977	1077	548	584	2703	2552	1284	638	637	10
11	1088	1080	797	589	583	1402	1118	896	583	583	2491	1852	1106	636	641	2452	2194	1278	692	701	11
12	1070	1073	851	859	671	1412	1124	959	670	696	2245	1958	1156	726	728	2723	2344	1333	780	784	12
13	1089	1100	914	763	788	1452	1133	1008	761	788	2307	2037	1221	804	814	2509	2325	1379	898	869	13
CONFIGURATION C																					
1	1101	1073	575	92	78	1241	1107	654	140	146	1610	1190	800	179	201	1987	1639	928	259	267	1
2	1102	1074	669	871	271	1254	1101	725	304	322	1646	1323	858	345	339	2015	1647	945	440	413	2
3	1112	1087	727	387	377	1258	1117	780	390	421	1603	1322	911	433	449	1994	1639	999	513	498	3
4	1115	1095	790	463	473	1233	1122	831	483	511	1625	1332	969	528	537	2000	1647	1045	596	582	4
5	1117	1096	845	572	585	1258	1128	892	585	627	1624	1321	1014	625	636	1990	1649	1096	683	675	5
6	1135	1115	963	784	778	1278	1132	1009	788	802	1560	1364	1126	798	813	2020	1701	1209	860	843	6
7	1142	1127	1091	971	991	1283	1167	1134	967	1003	1682	1374	1241	894	1003	2029	1718	1310	1027	1026	7
8	1089	1089	501	64	85	1402	1088	567	96	119	2121	1670	806	130	188	2312	2200	993	324	233	8

NACA

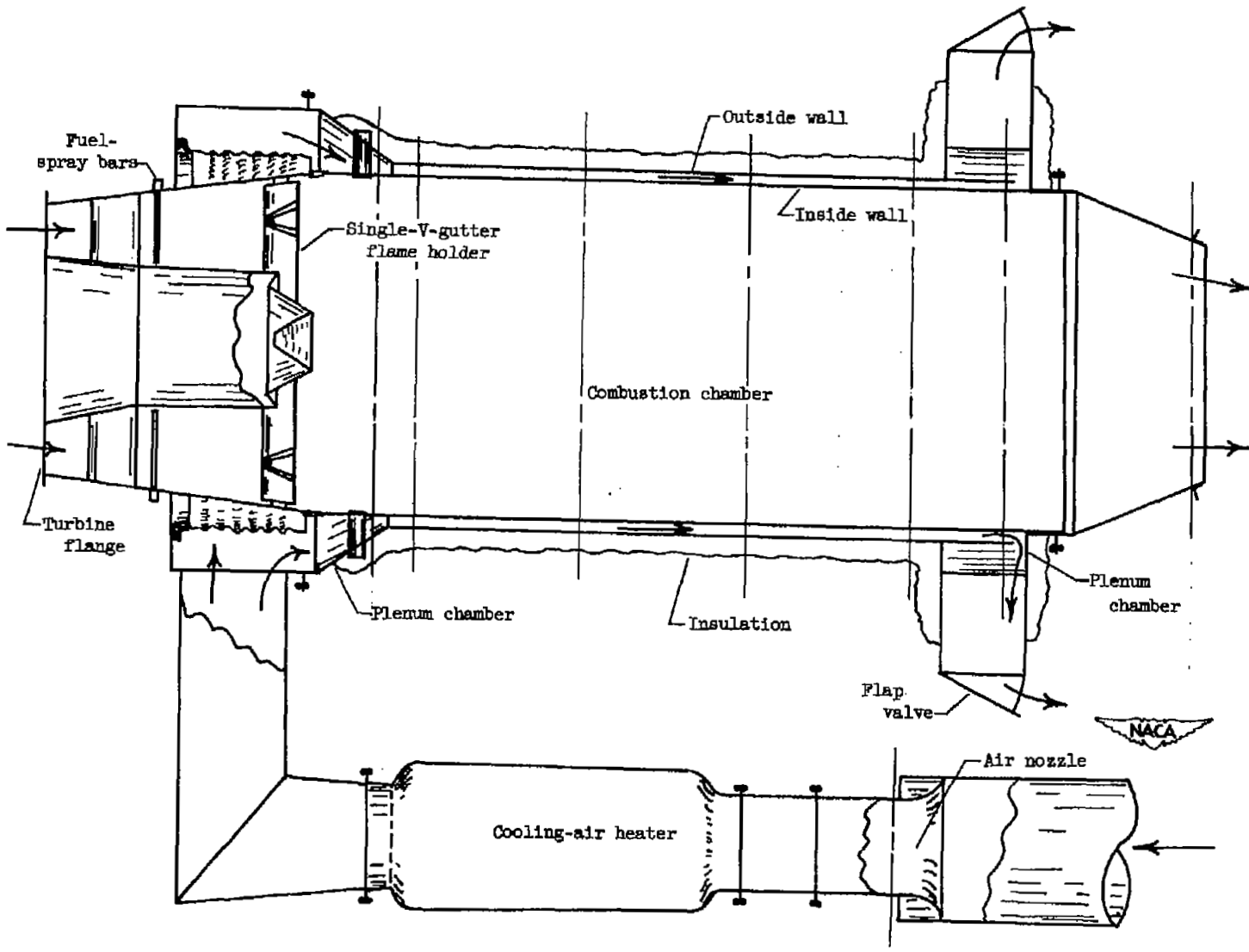
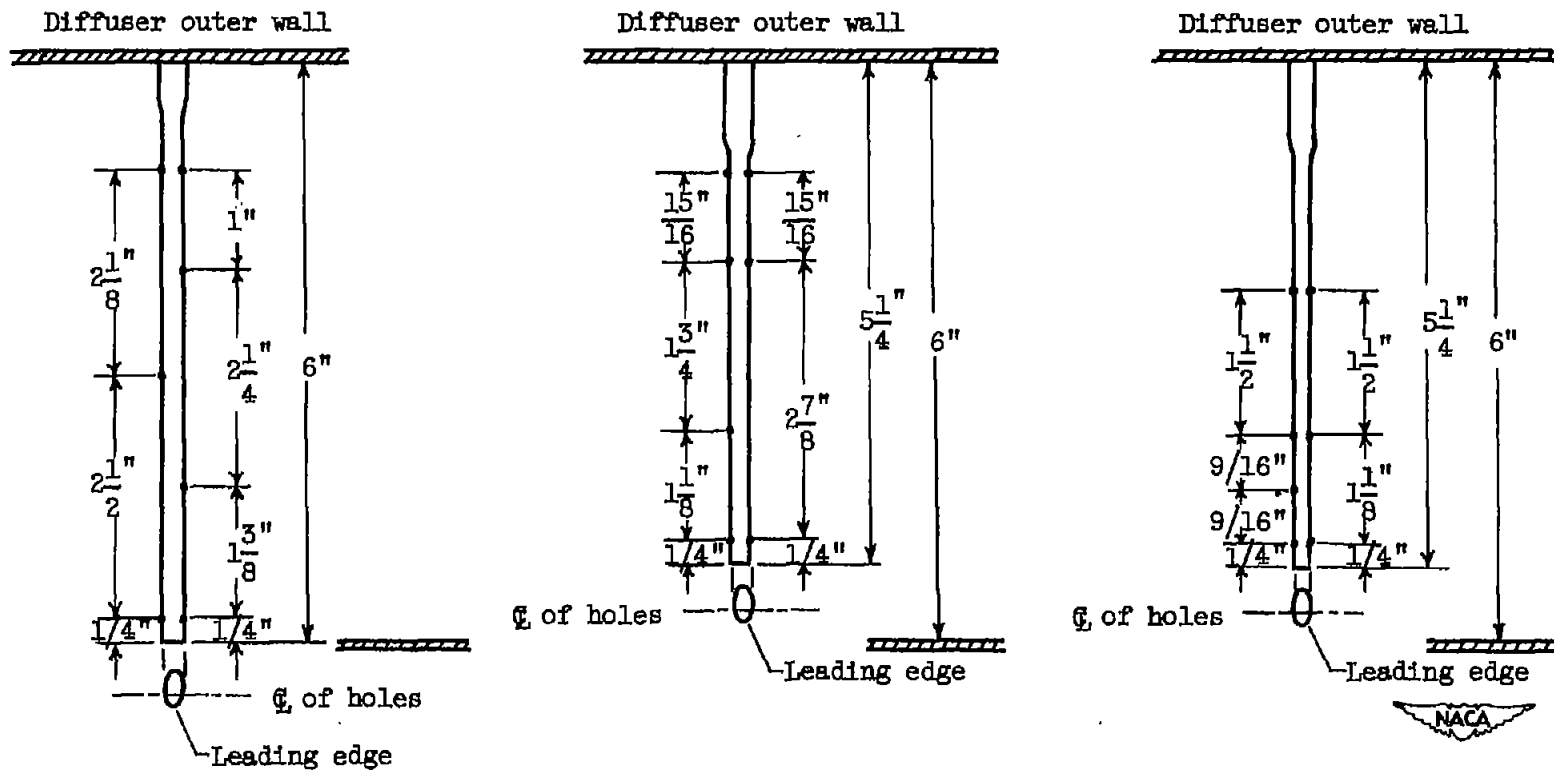


Figure 1. - Tail-pipe burner assembly.



(a) Nearly uniform fuel distribution.

(b) Fuel distribution concentrated toward outside of burner.

(c) Fuel distribution concentrated toward center of burner.

Figure 2. - Fuel-spray bars.

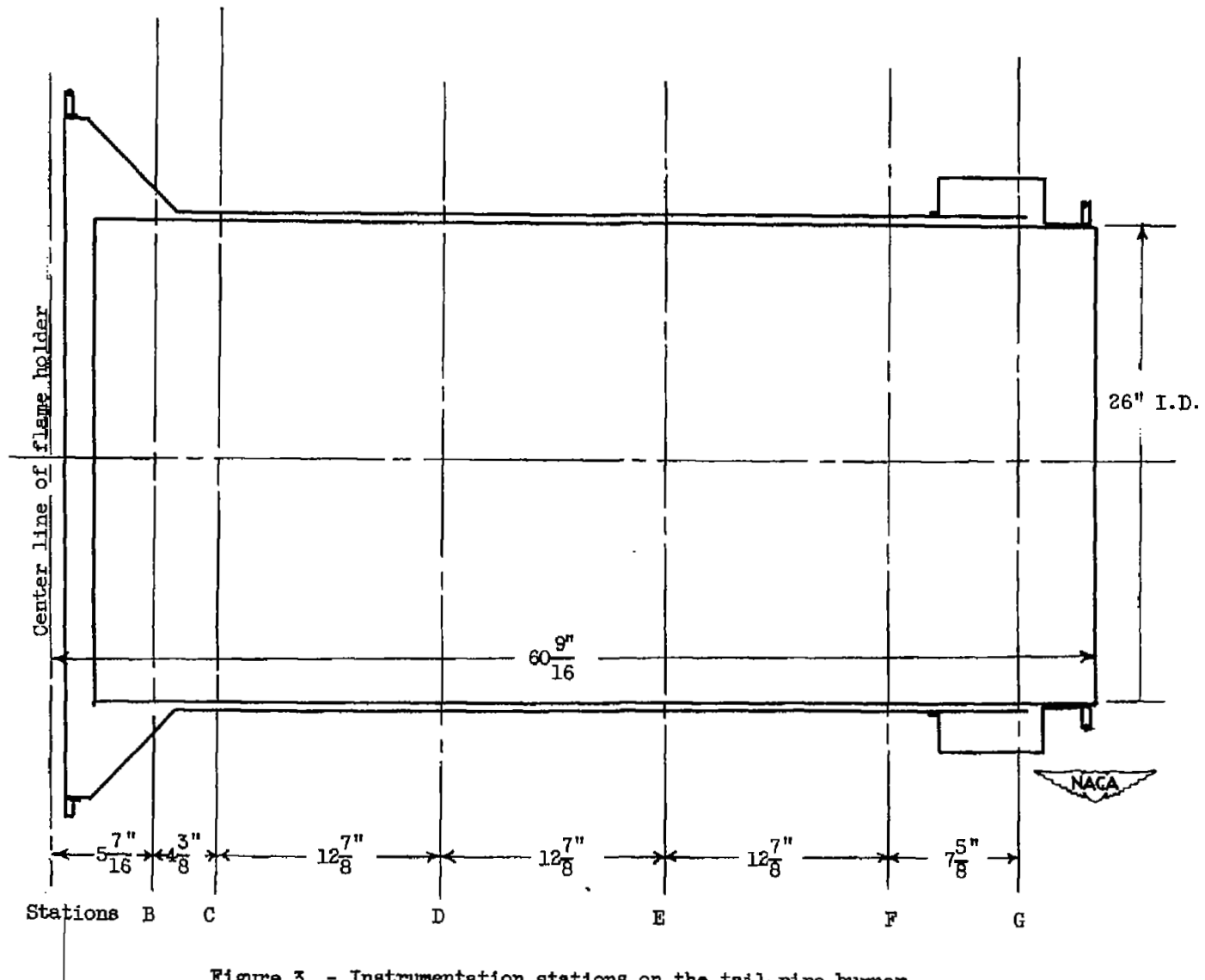
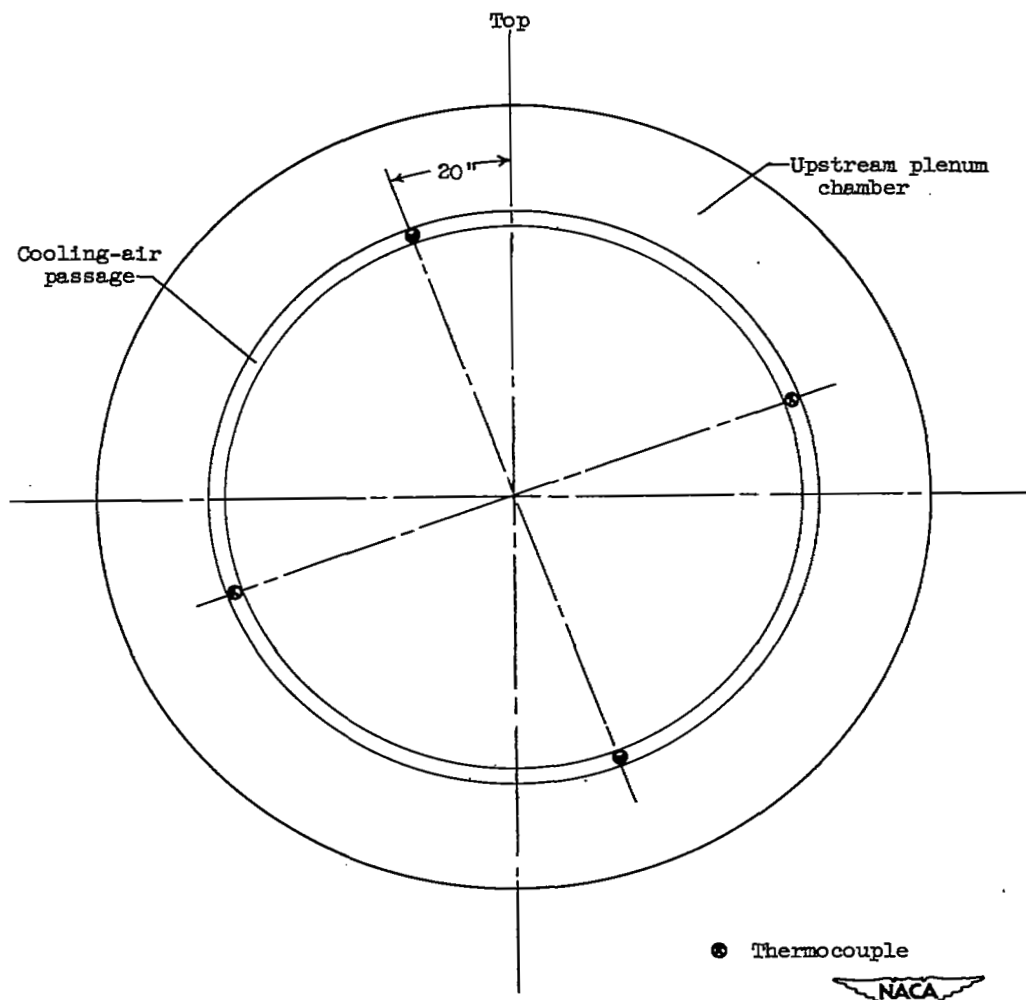


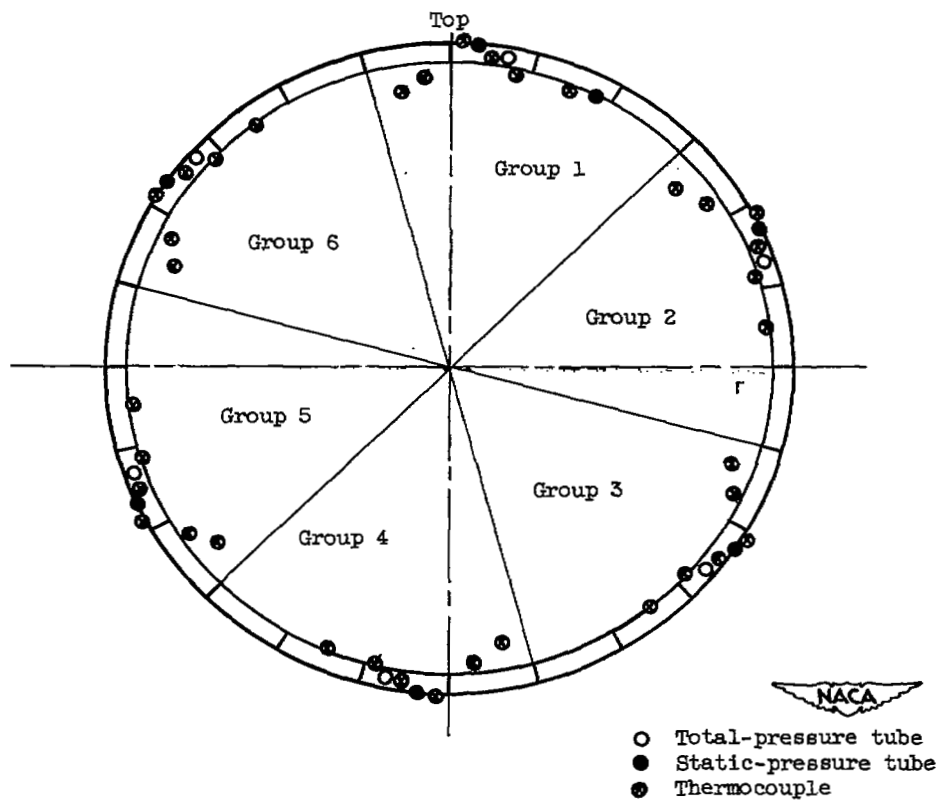
Figure 3. - Instrumentation stations on the tail-pipe burner.

2408



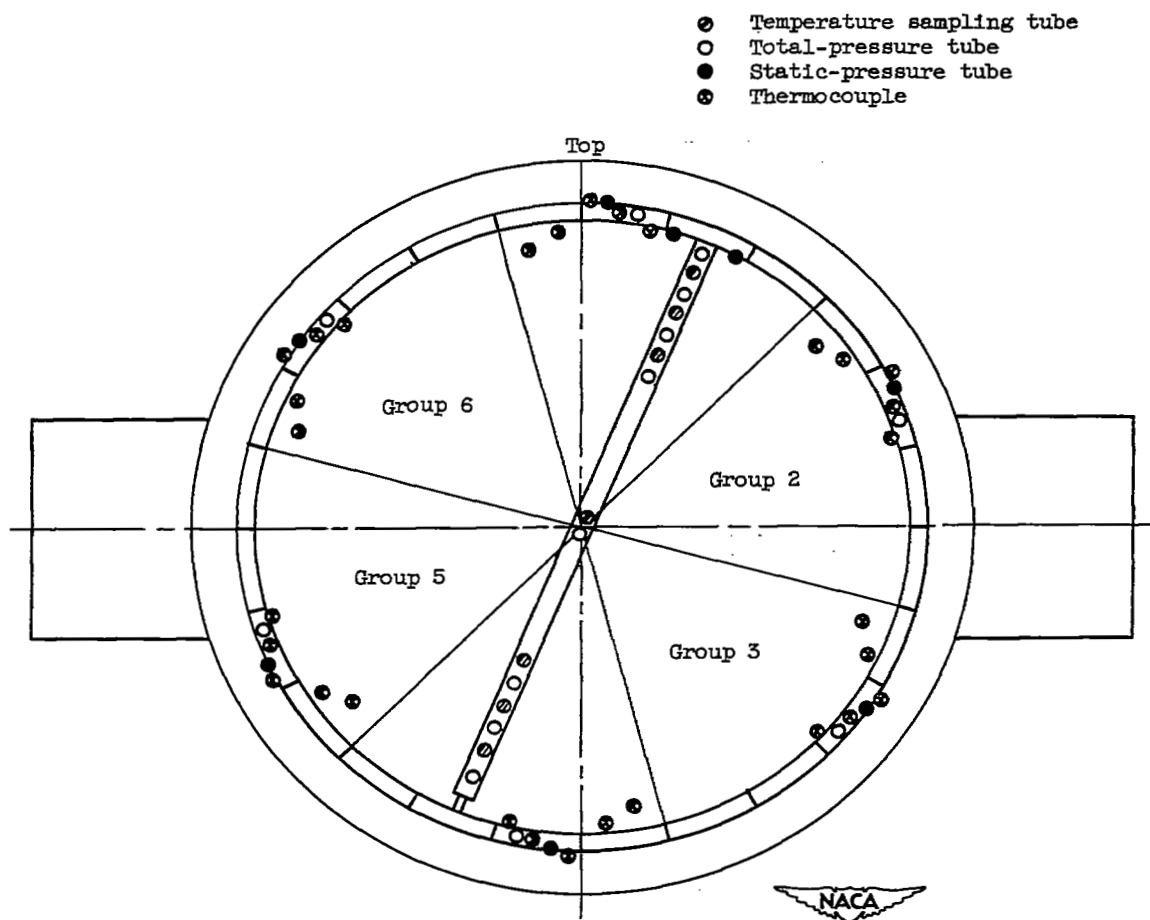
(a) Station B, cooling-passage inlet, looking downstream.

Figure 4. - Location of instrumentation.



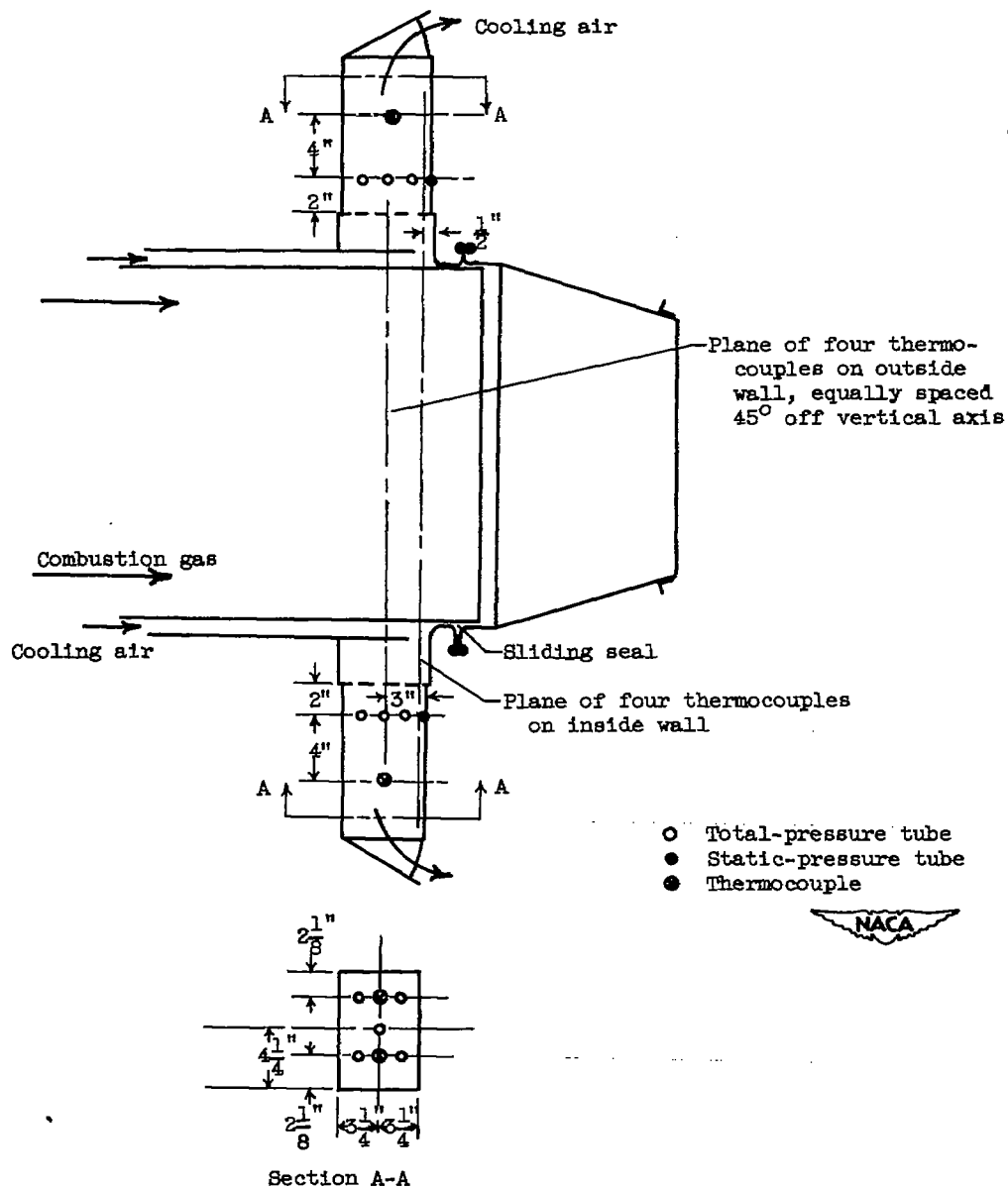
(b) Stations C through E, looking downstream.

Figure 4. - Continued. Location of instrumentation.



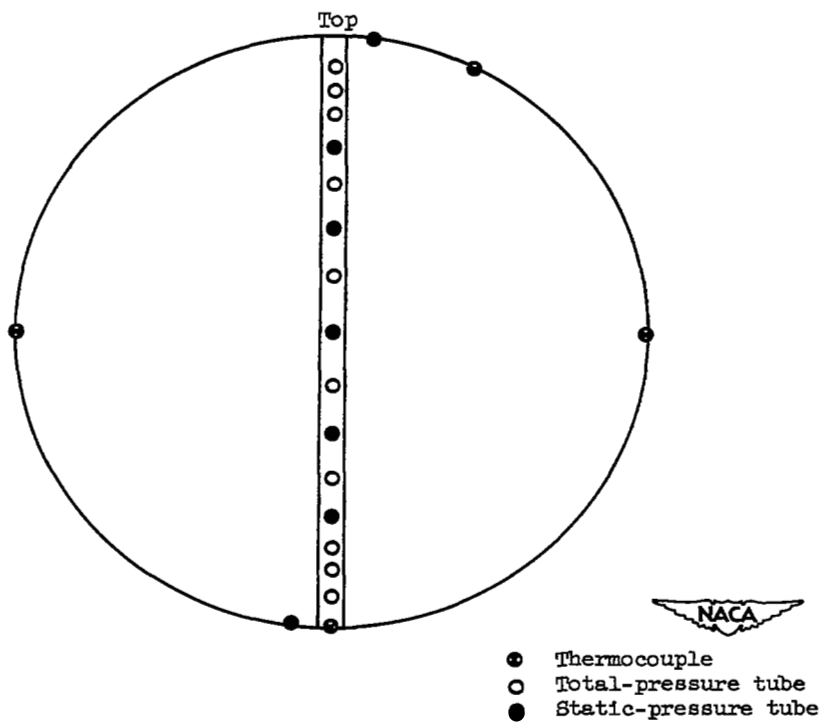
(c) Station F, looking downstream.

Figure 4. - Continued. Location of instrumentation.



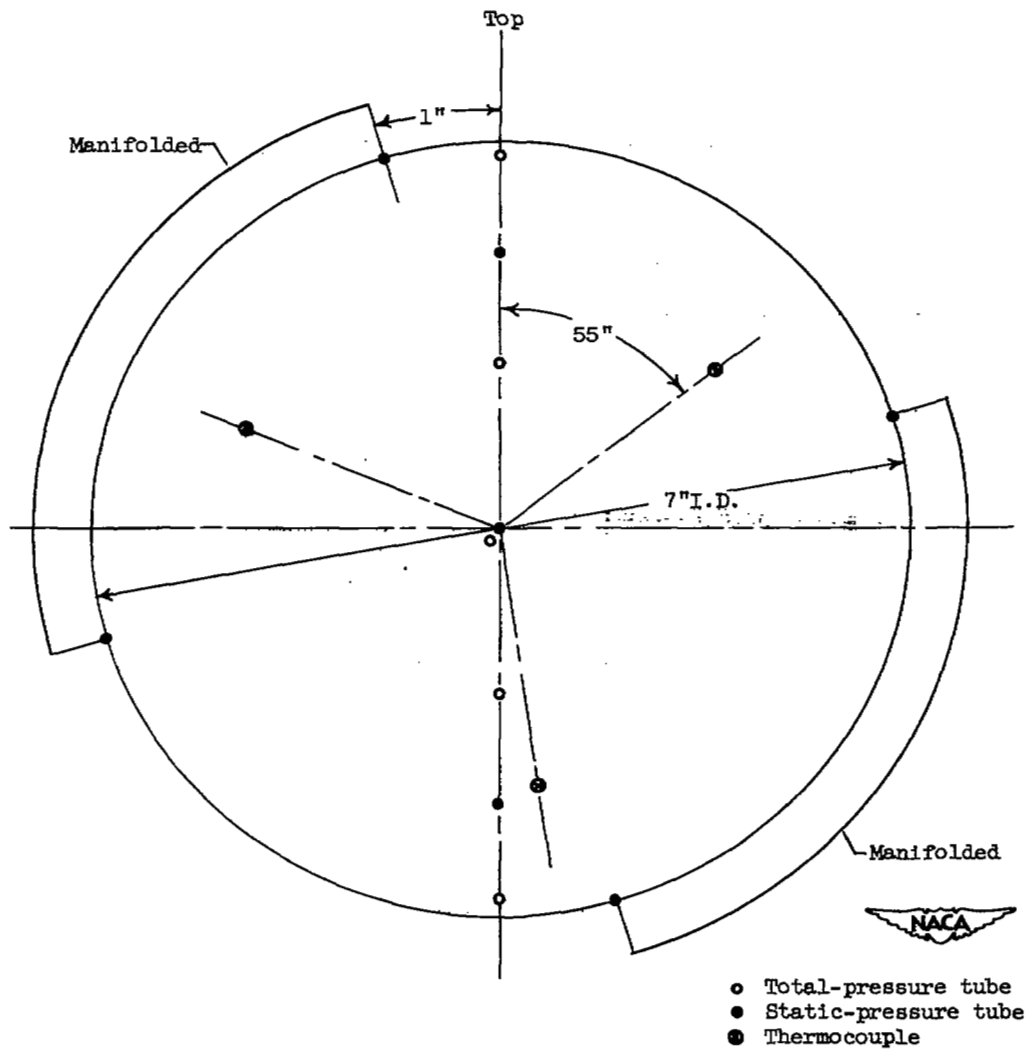
(d) Station G.

Figure 4. - Continued. Location of instrumentation.



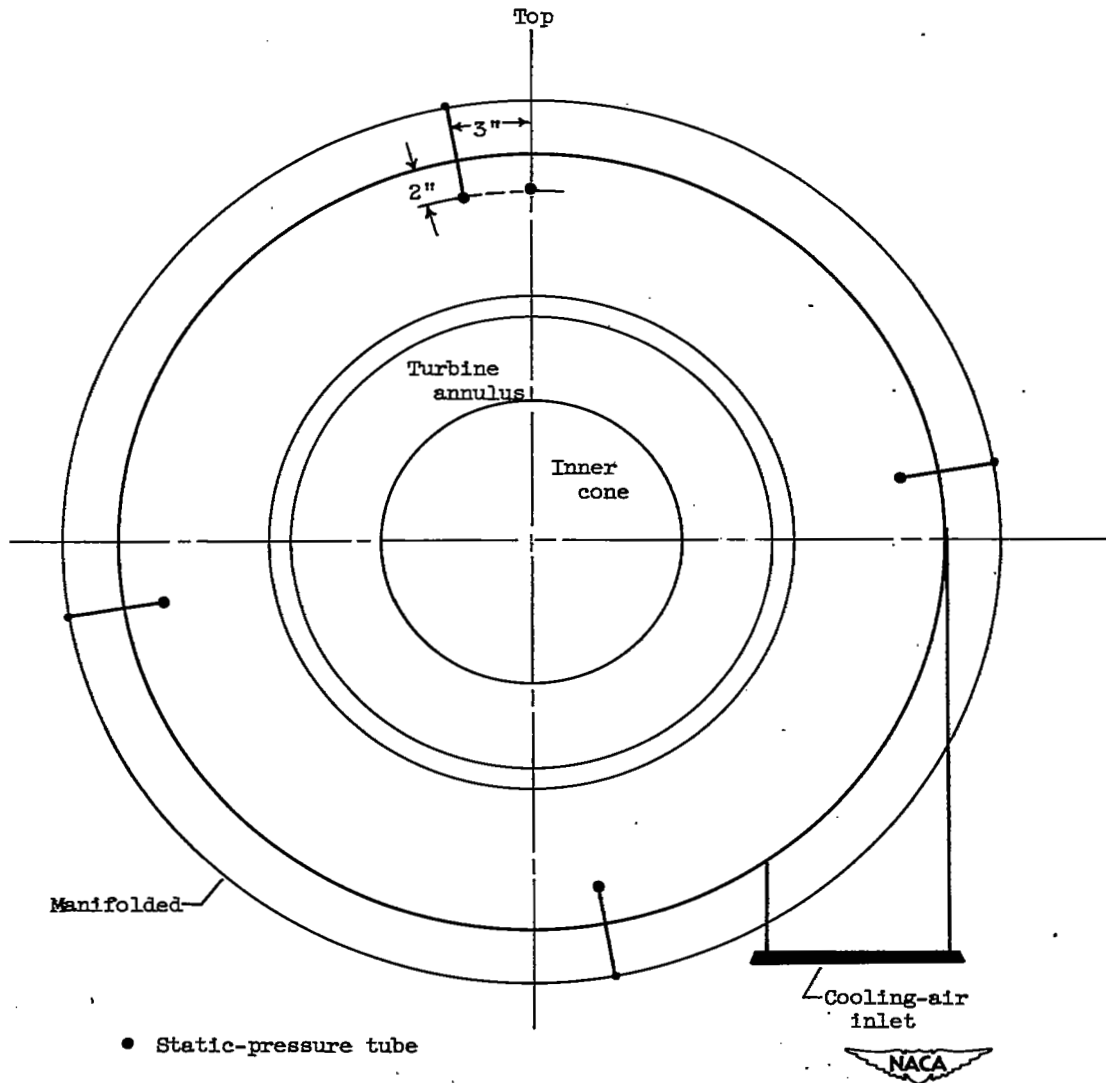
(e) Exhaust-nozzle exit, looking downstream.

Figure 4. - Continued. Location of instrumentation.



(f) Throat of cooling-air metering nozzle.

Figure 4. - Continued. Location of instrumentation.



(g) Cooling-air inlet plenum chamber, looking downstream.

Figure 4. - Concluded. Location of instrumentation.

2408

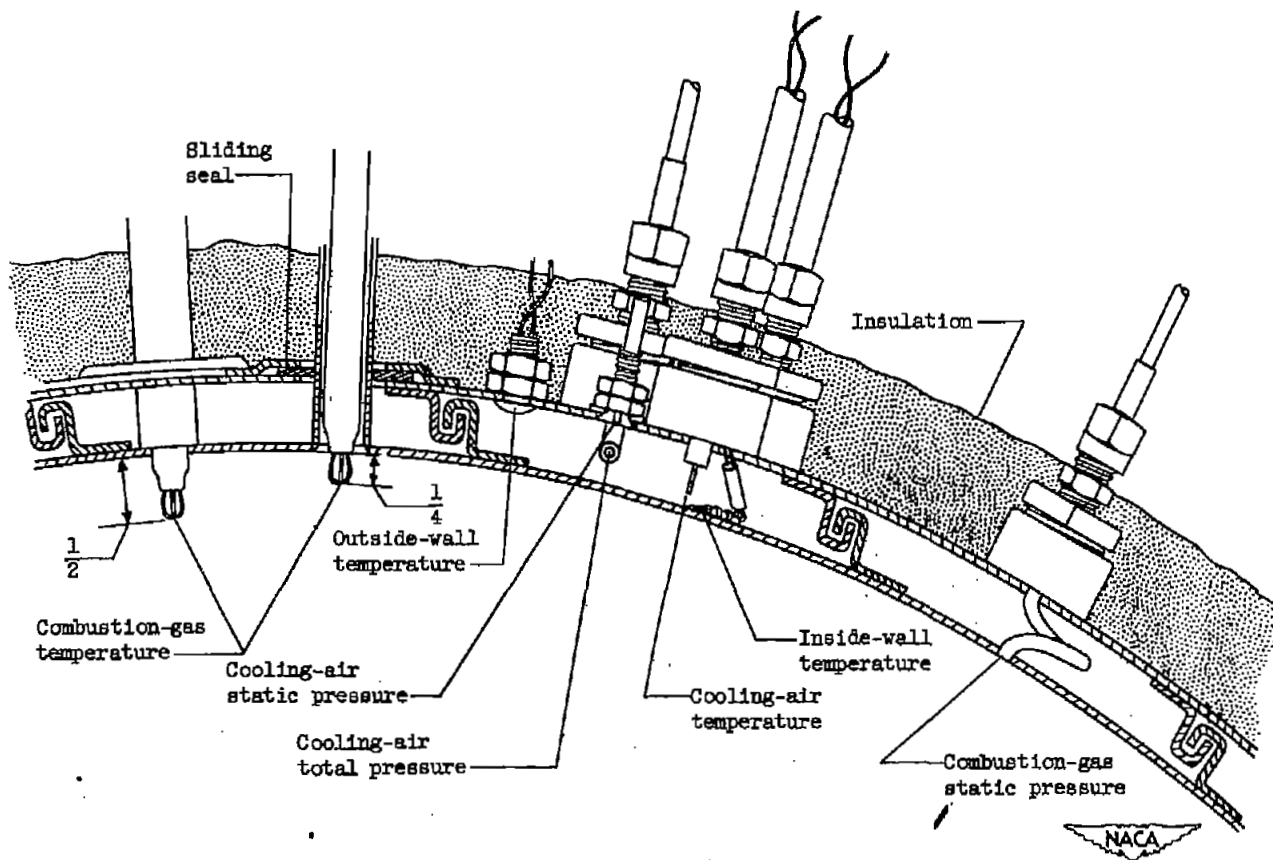


Figure 5. - Typical instrumentation group for stations C to F.

2408

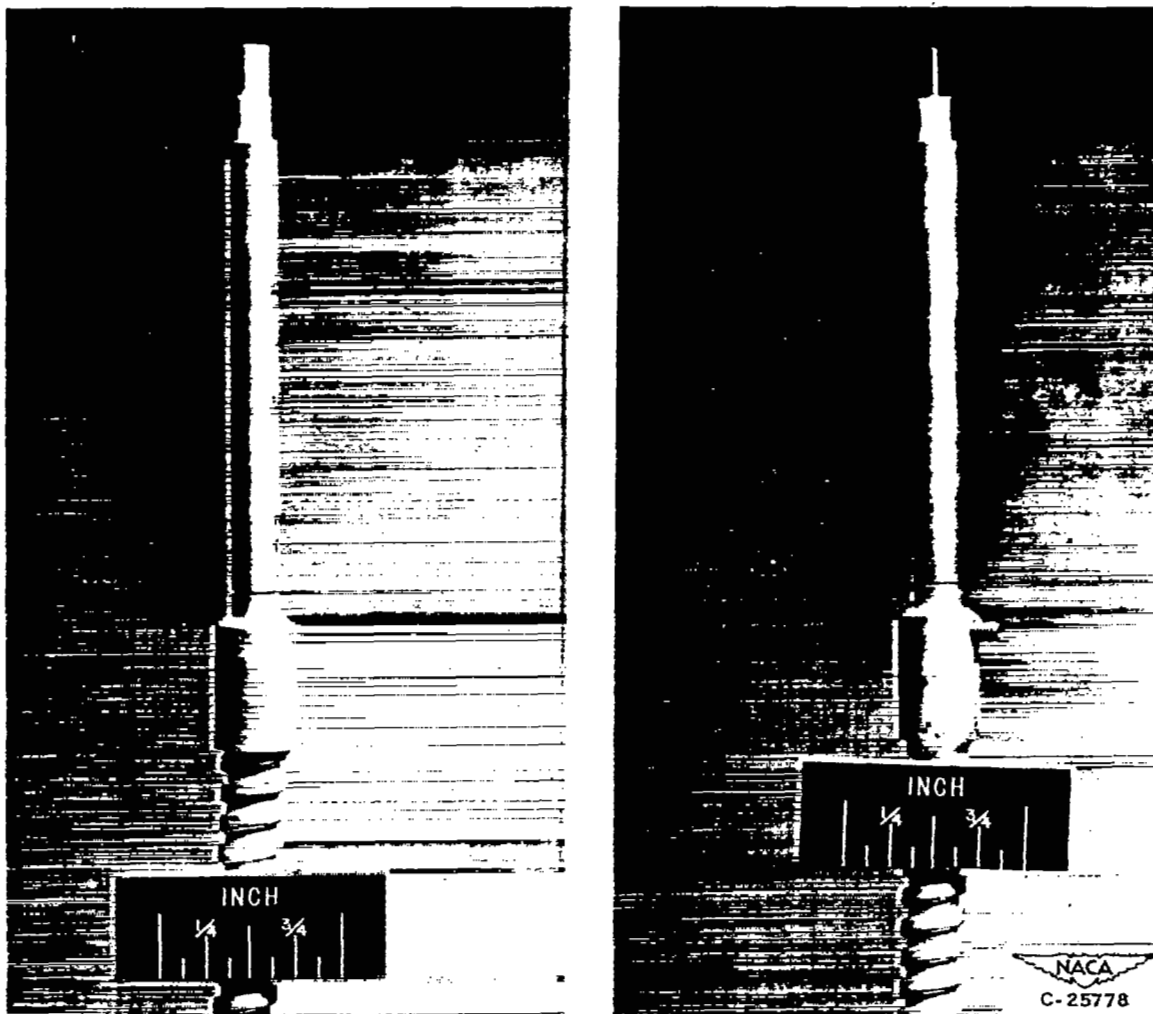
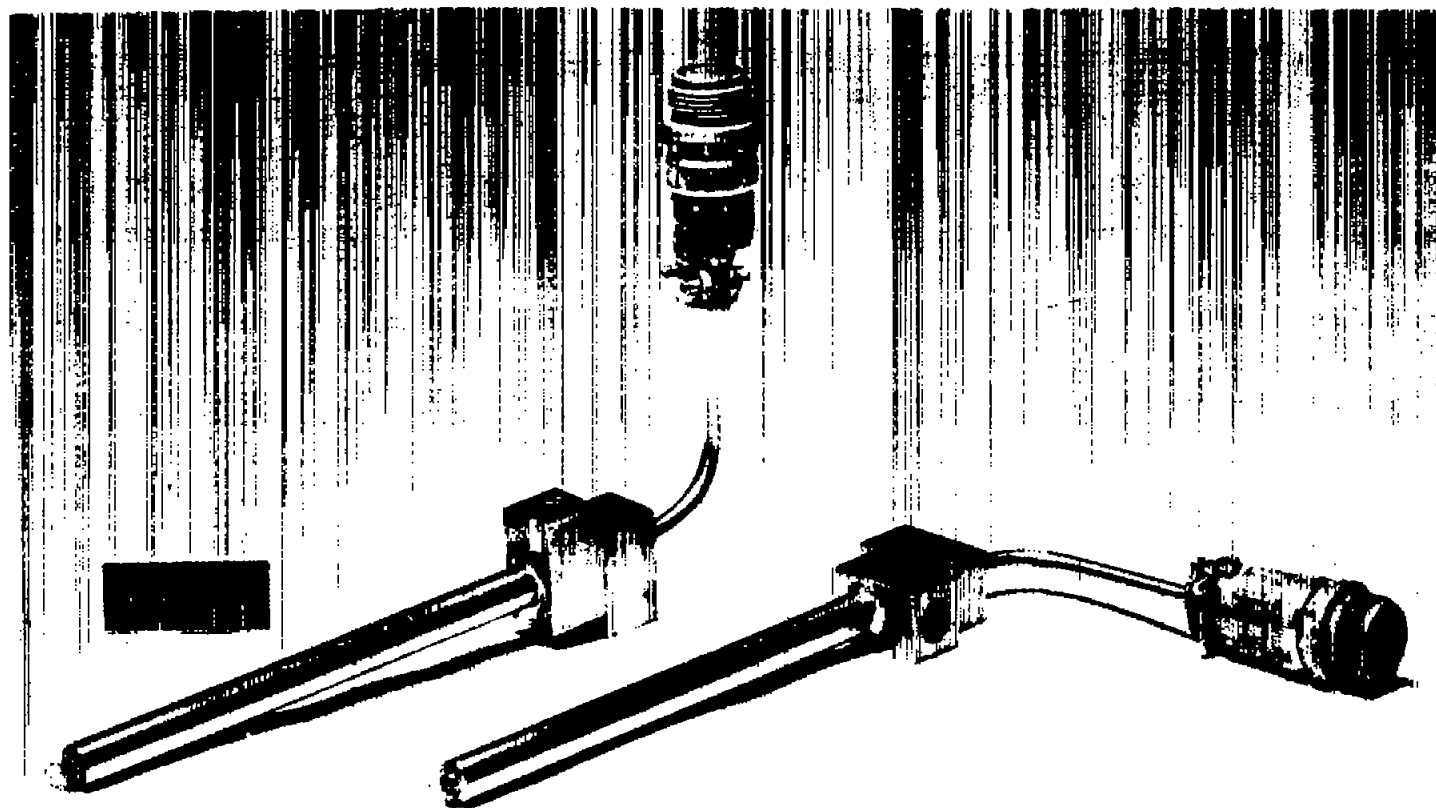


Figure 6. - National Bureau of Standards type shielded thermocouple for cooling-air temperature measurement.



NACA
C-26128

Figure 7. - Platinum-rhodium - platinum thermocouple probes.

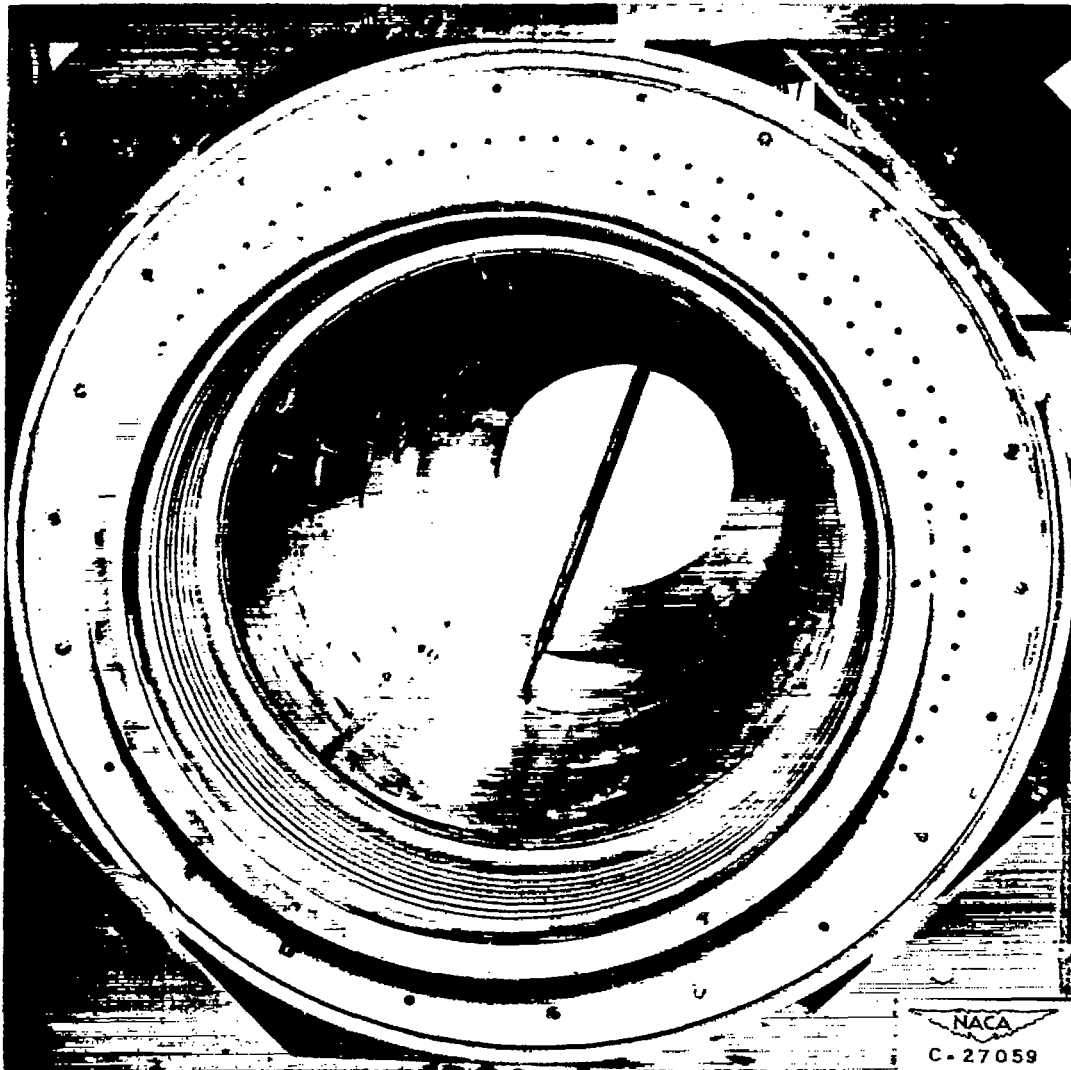
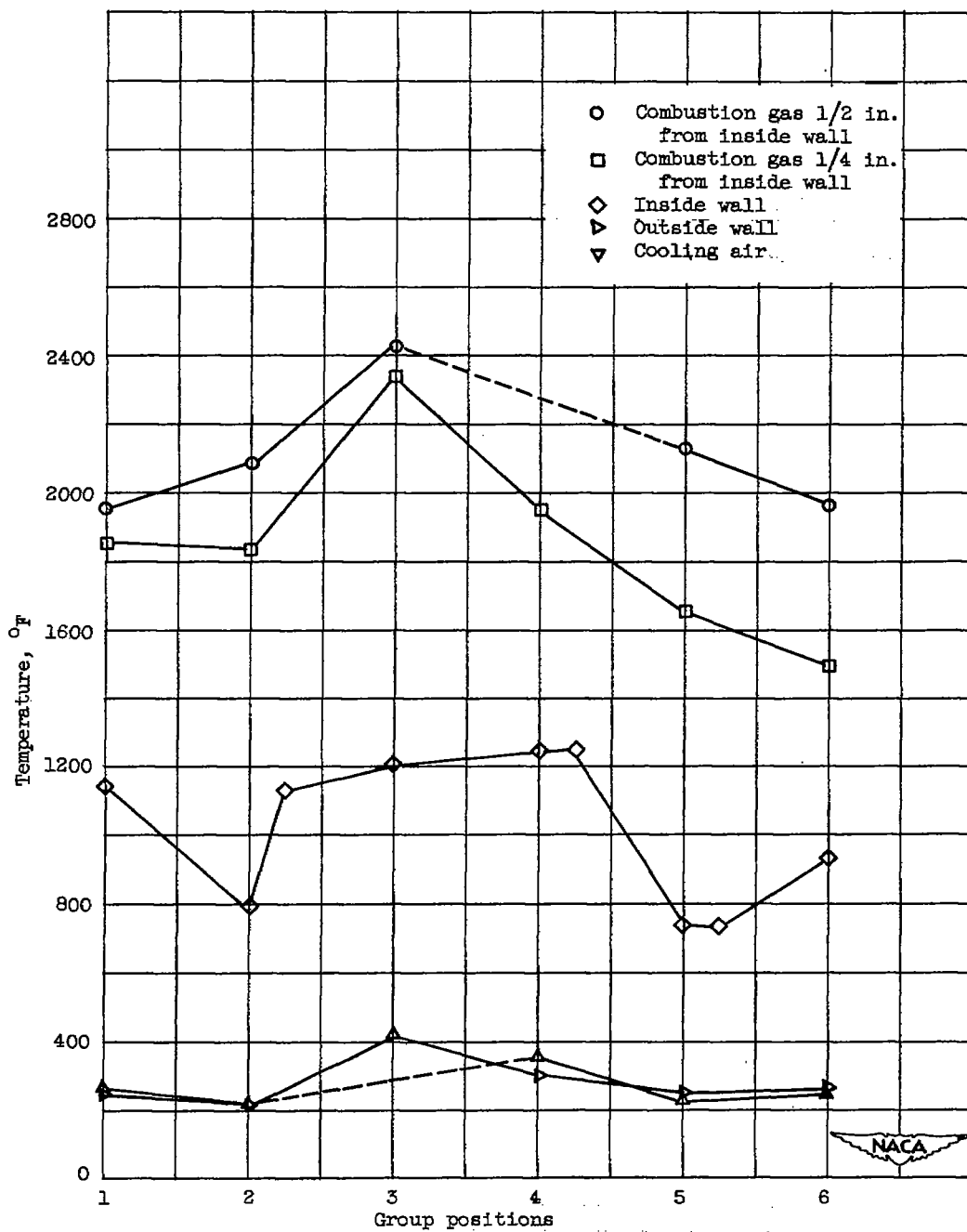
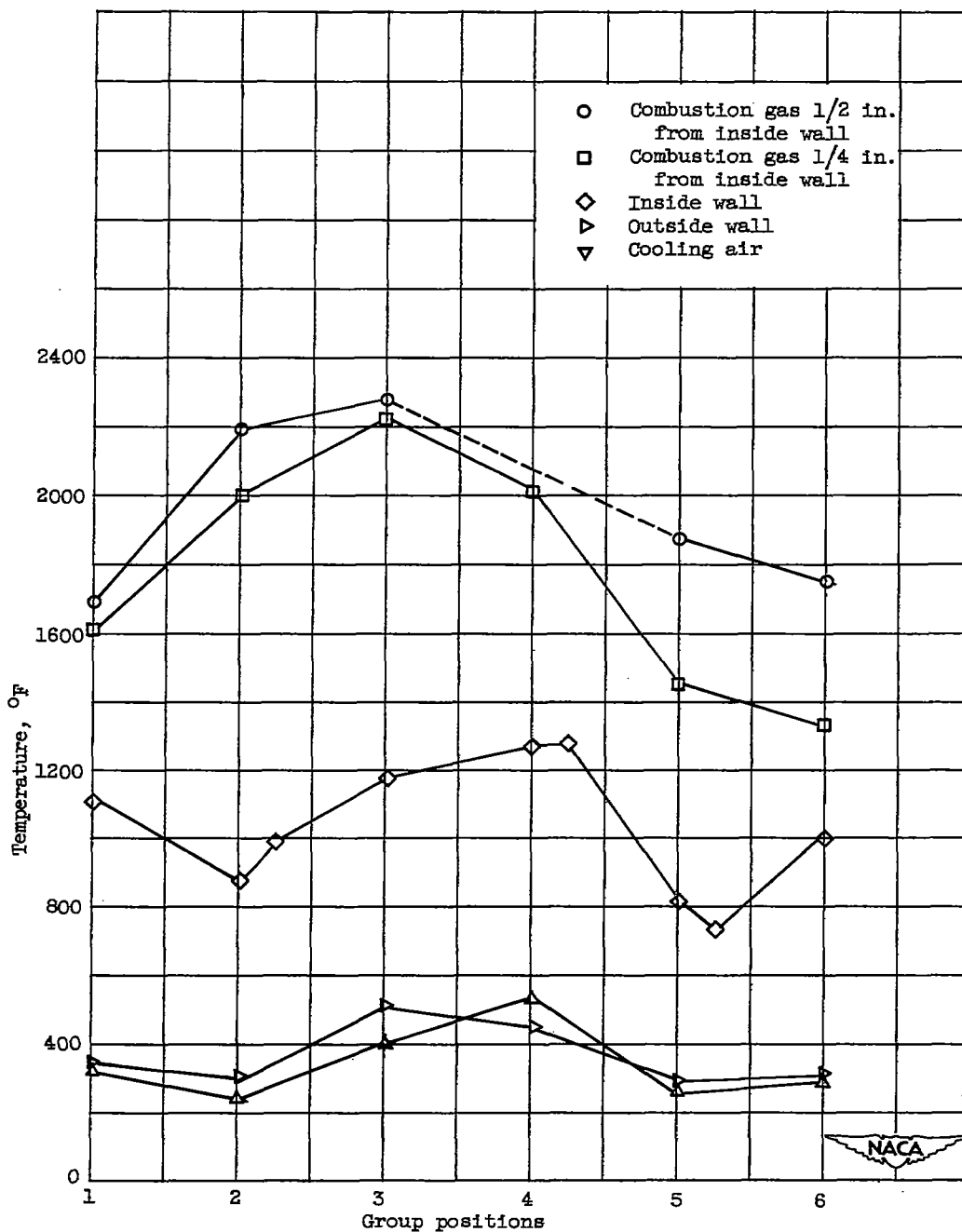


Figure 8. - Interior view of combustion chamber showing installation of sonic-flow orifice rake and platinum-rhodium - platinum thermocouples.



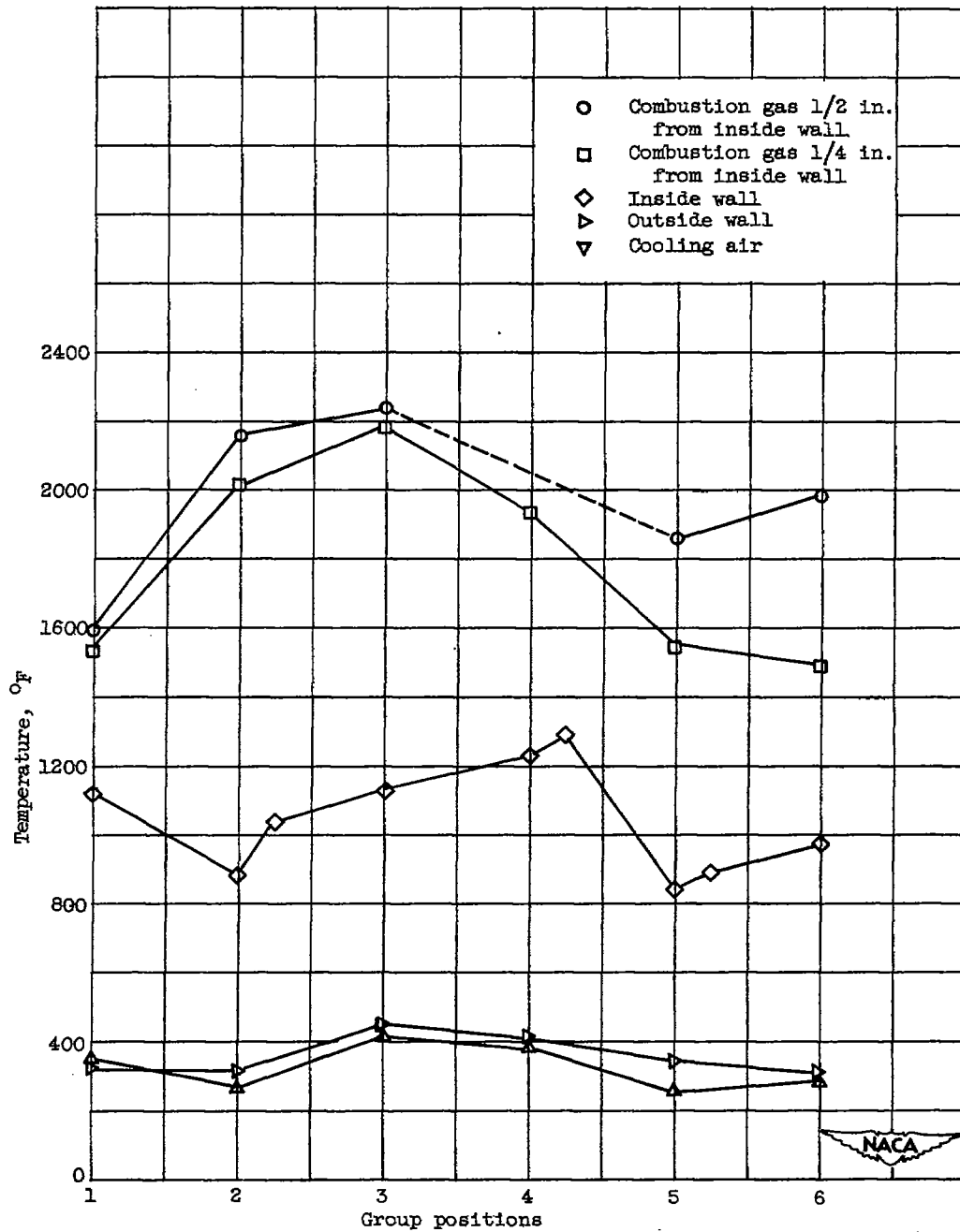
(a) Accumulated afterburner time, 32 minutes; exhaust-gas total temperature, 2993° R; mass-flow ratio, 0.1006; inlet cooling-air temperature, 526° R.

Figure 9. - Circumferential temperature variations at station F, configuration A.



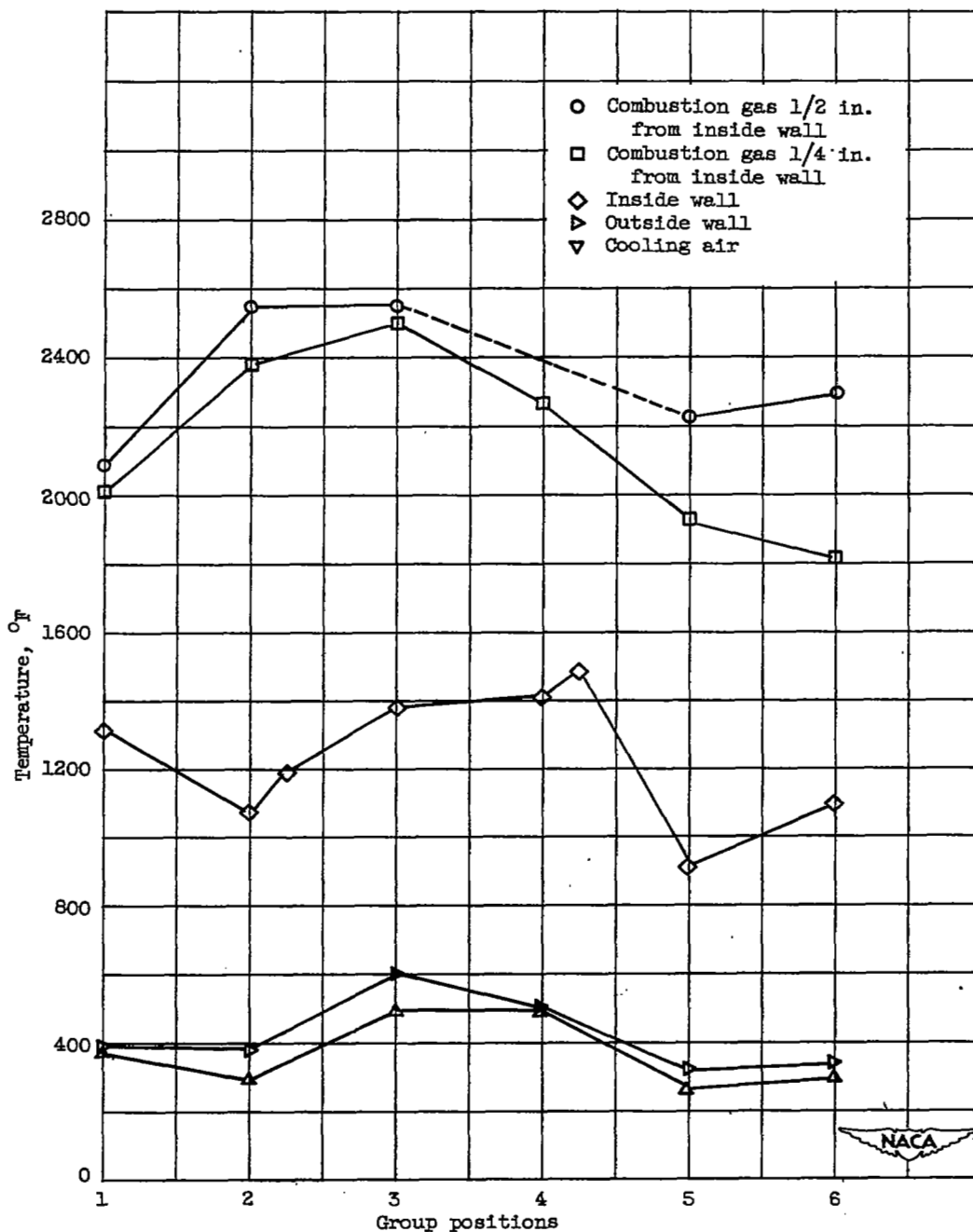
(b) Accumulated afterburner time, 3 hours and 36 minutes; exhaust-gas total temperature approximately 3060° R; mass-flow ratio; 0.0949; inlet cooling-air temperature, 536° R.

Figure 9. - Continued. Circumferential temperature variations at station F, configuration A.



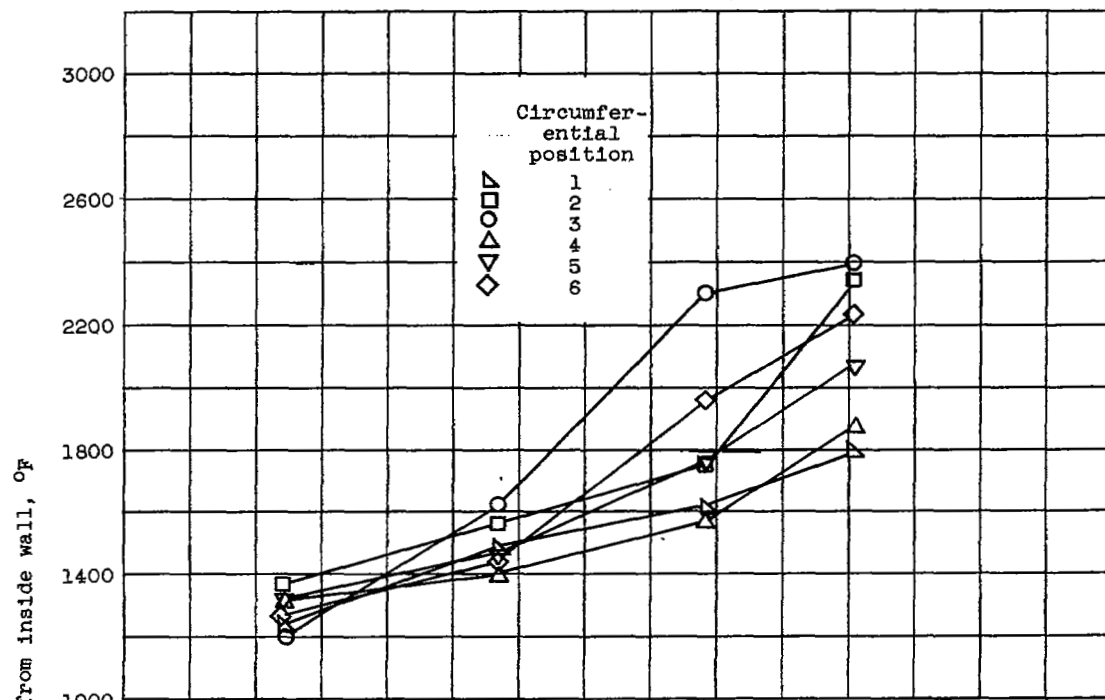
(c) Accumulated afterburner time, 9 hours and 22 minutes; exhaust-gas total temperature, 3102° R; mass-flow ratio, 0.0985; inlet cooling-air temperature, 529° R.

Figure 9. - Continued. Circumferential temperature variations at station F, configuration A.

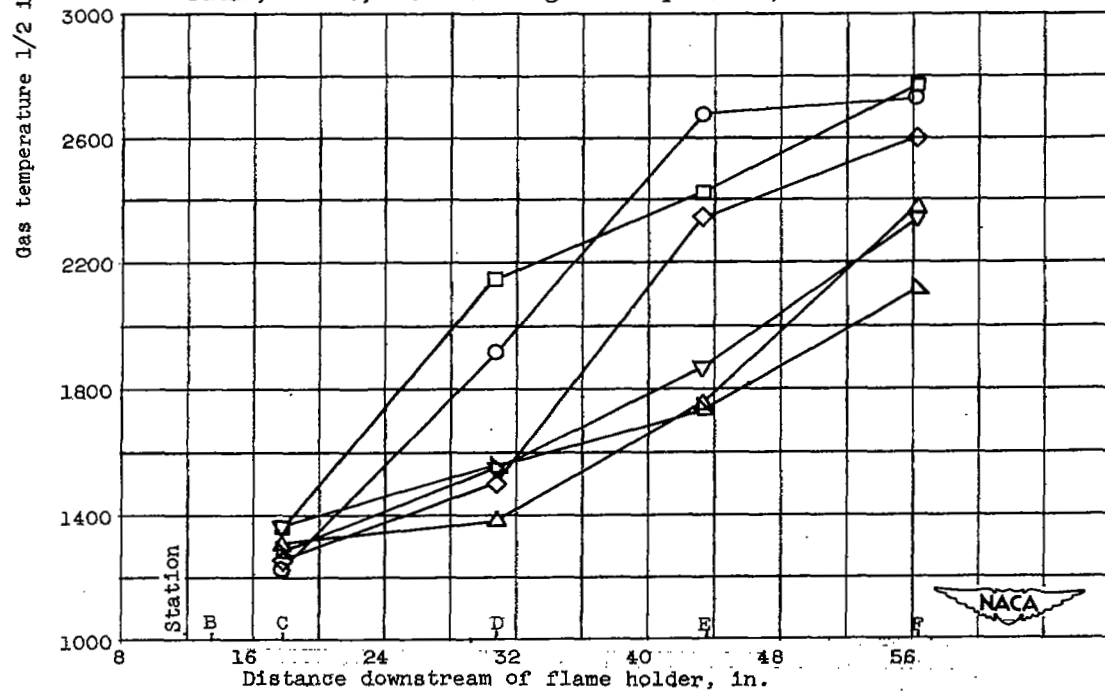


(d) Accumulated afterburner time, 3 hours and 48 minutes; exhaust-gas total temperature, 3484° R; mass-flow ratio, 0.1050; inlet cooling-air temperature, 530° R.

Figure 9. - Concluded. Circumferential temperature variations at station F, configuration A.



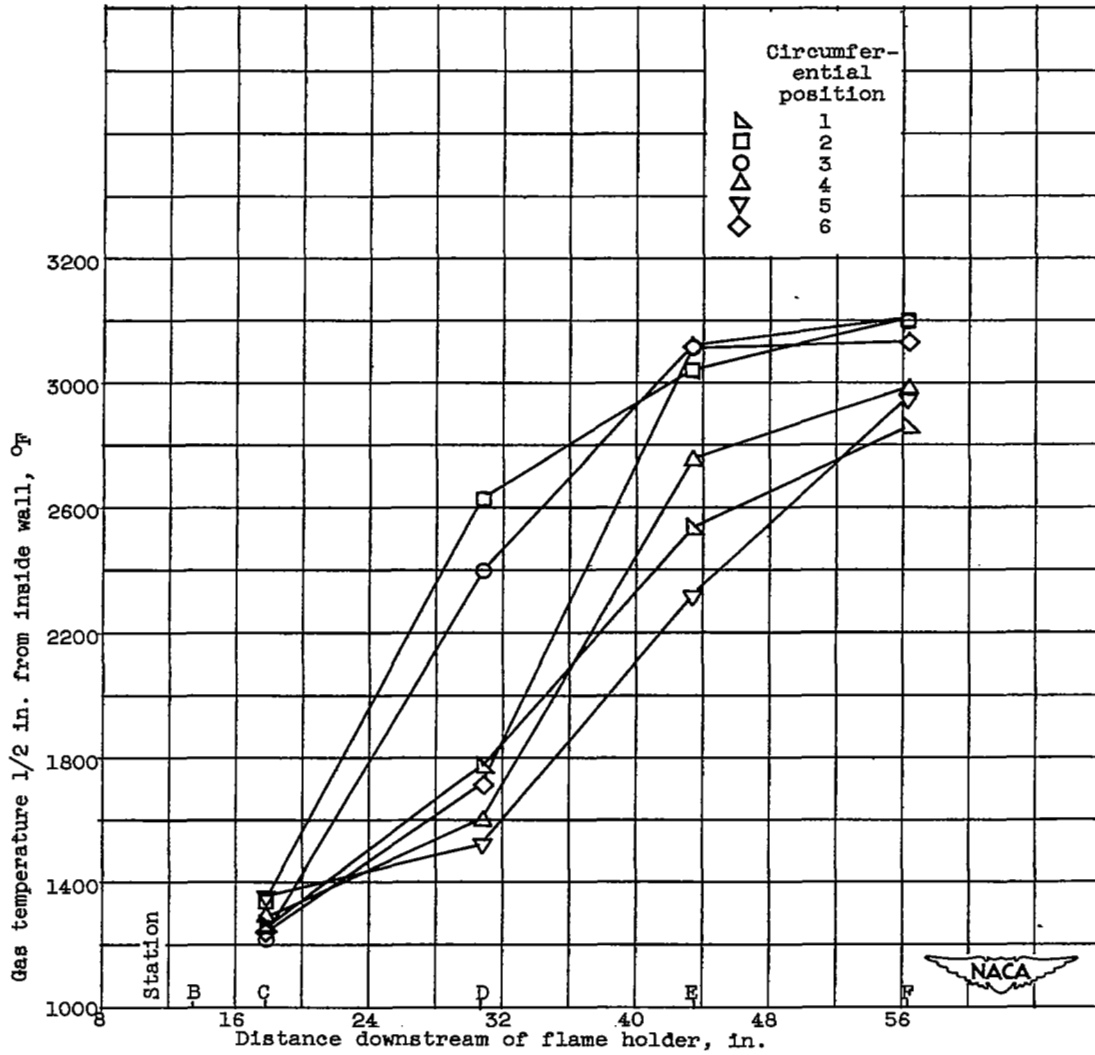
(a) Exhaust-gas total temperature, 3067° R; mass-flow ratio, 0.1426; inlet cooling-air temperature, 1033° R.



(b) Exhaust-gas total temperature, 3394° R; mass-flow ratio, 0.1436; inlet cooling-air temperature, 539° R.

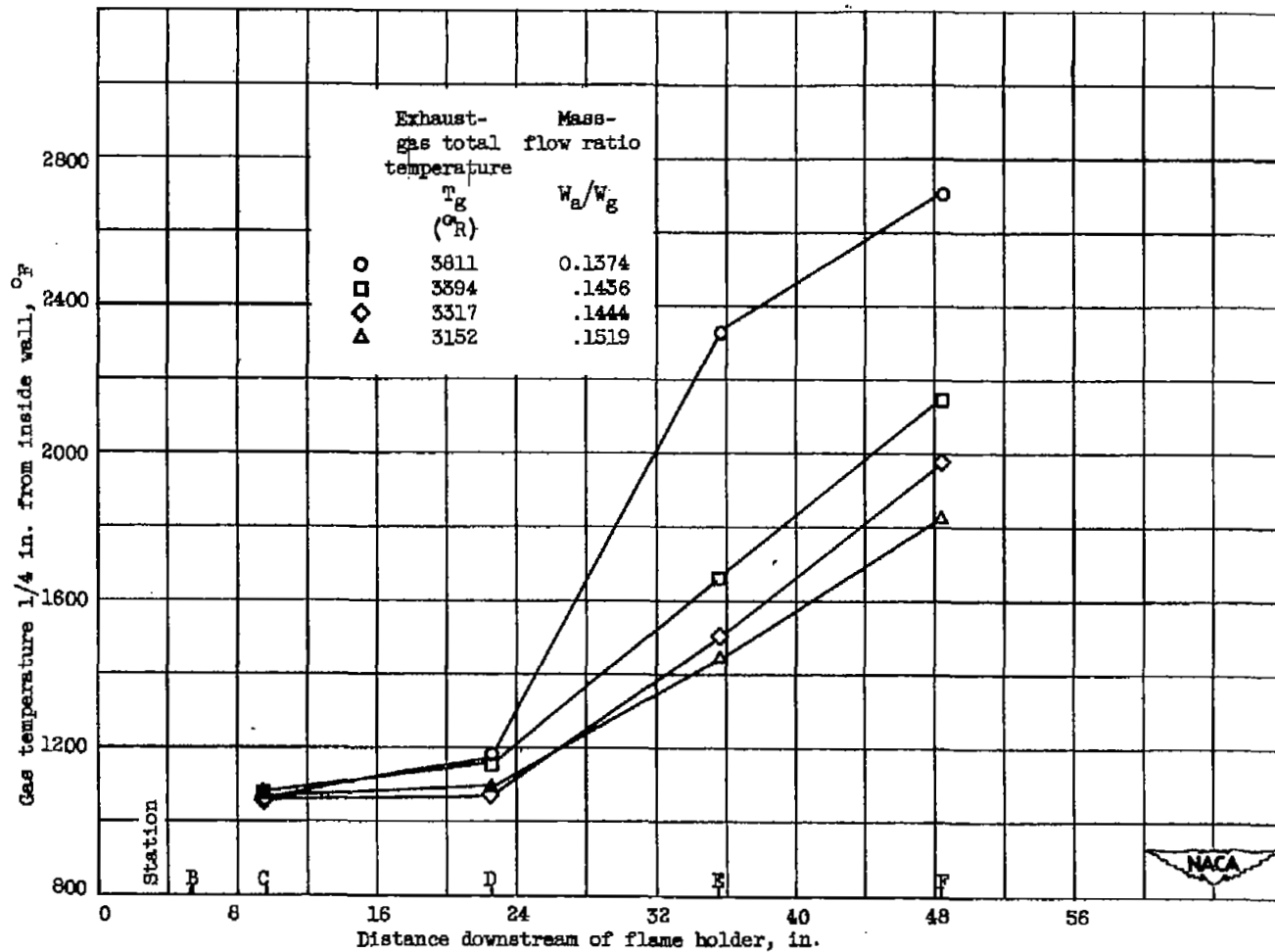
Figure 10. - Longitudinal gas-temperature profiles 1/2 inch from inside wall, configuration A.

2408



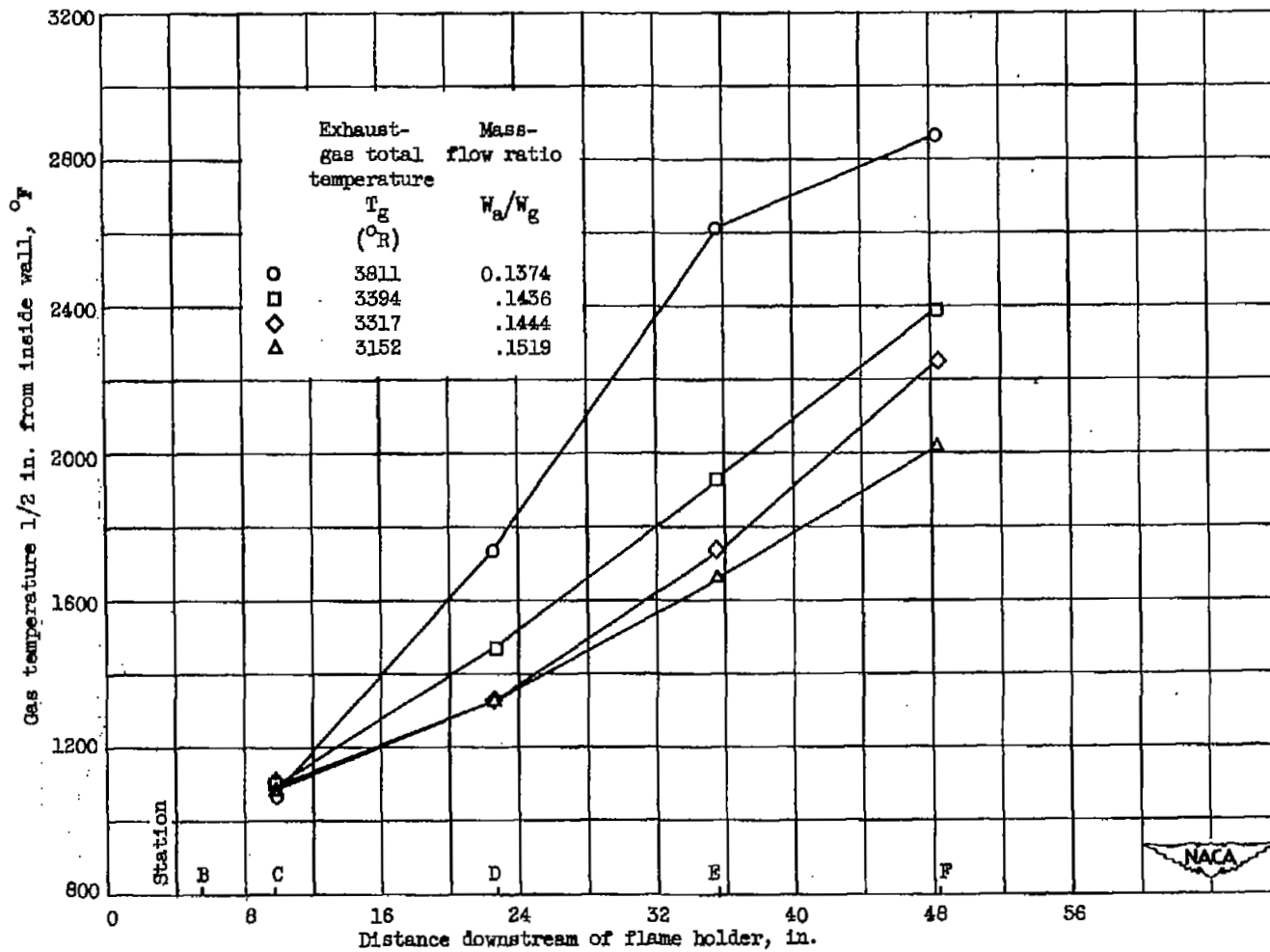
(c) Exhaust-gas total temperature, 3811° R; mass-flow ratio, 0.1374; inlet cooling-air temperature, 538° R.

Figure 10. - Concluded. Longitudinal gas-temperature profiles 1/2 inch from inside wall, configuration A.



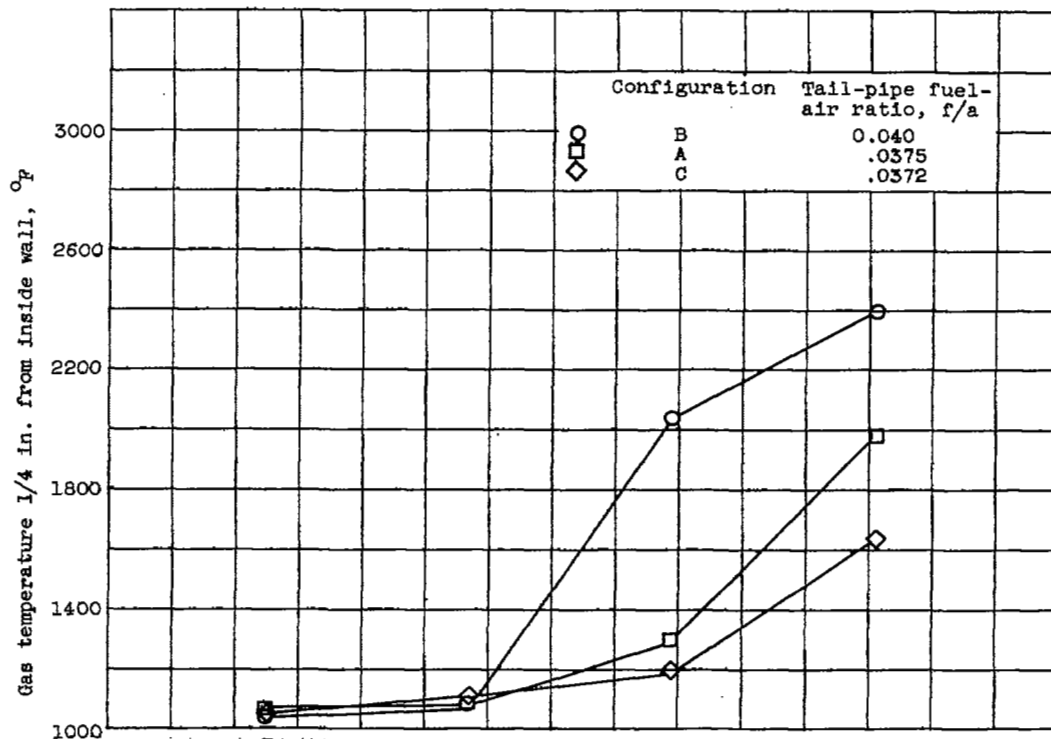
(a) Temperature 1/4 inch from inside wall.

Figure 11. - Variation of longitudinal profile of exhaust-gas temperature near inside wall with exhaust-gas temperature for configuration A. Approximate inlet cooling-air temperature, $520^{\circ}R$.

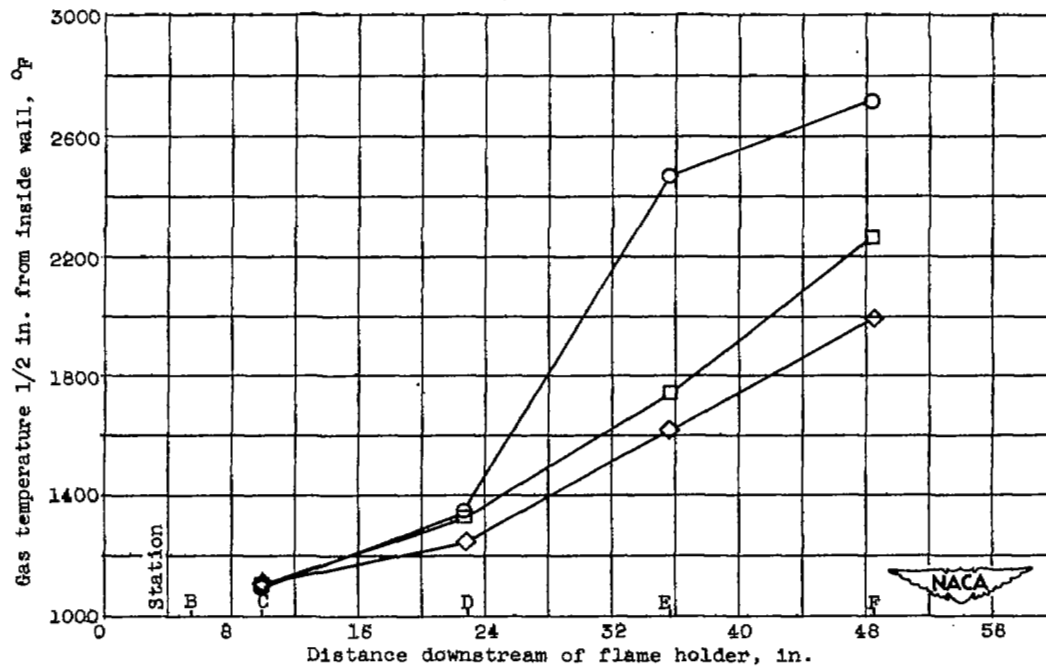


(b) Temperature 1/2 inch from inside wall.

Figure 11. - Concluded. Variation of longitudinal profile of exhaust-gas temperature near inside wall with exhaust-gas temperature for configuration A. Approximate inlet cooling-air temperature, $520^{\circ}R$.



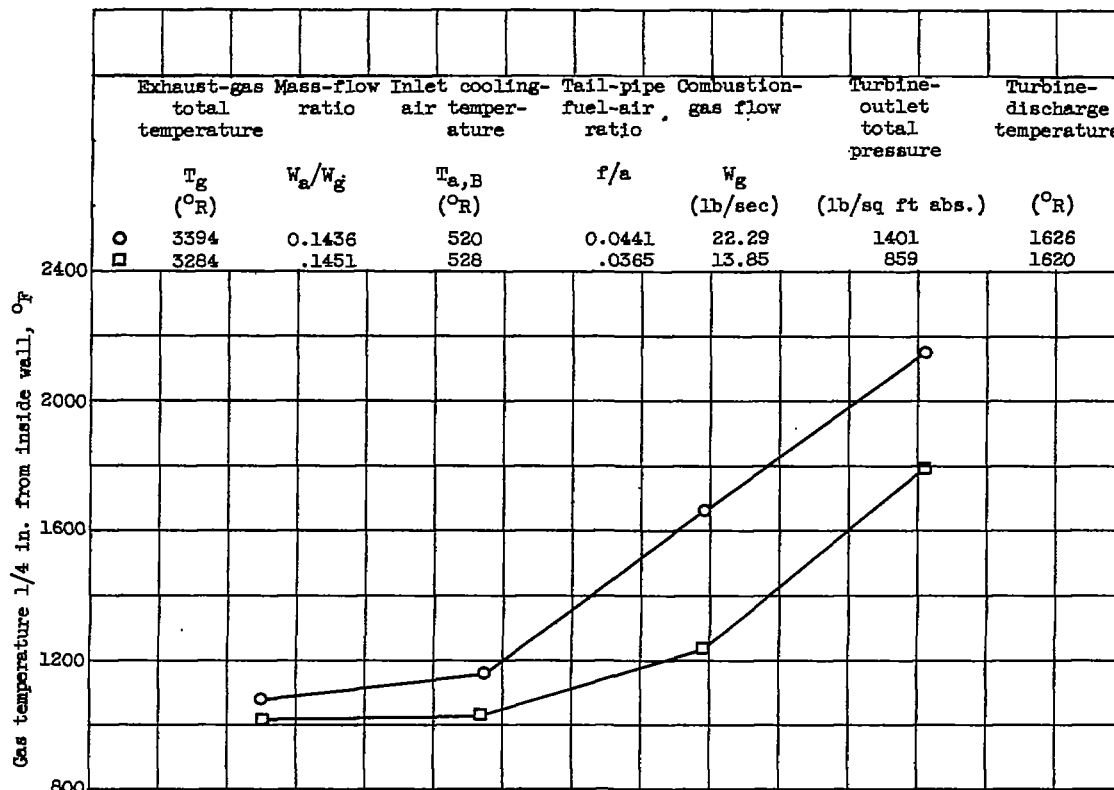
(a) Temperatures 1/4 inch from inside wall.



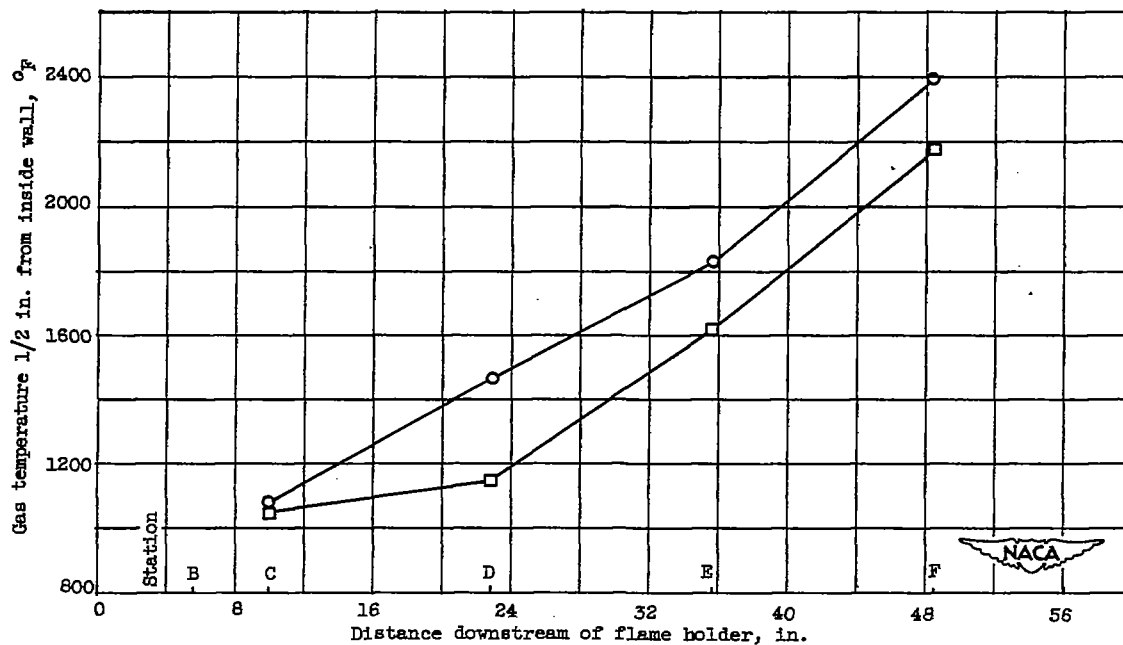
(b) Temperatures 1/2 inch from inside wall.

Figure 12. - Effect of fuel distribution on gas temperatures near inside wall. Exhaust-gas total temperature, approximately 3230° R; mass-flow ratio, 0.145; cooling-air inlet temperature, 510° R.

2408



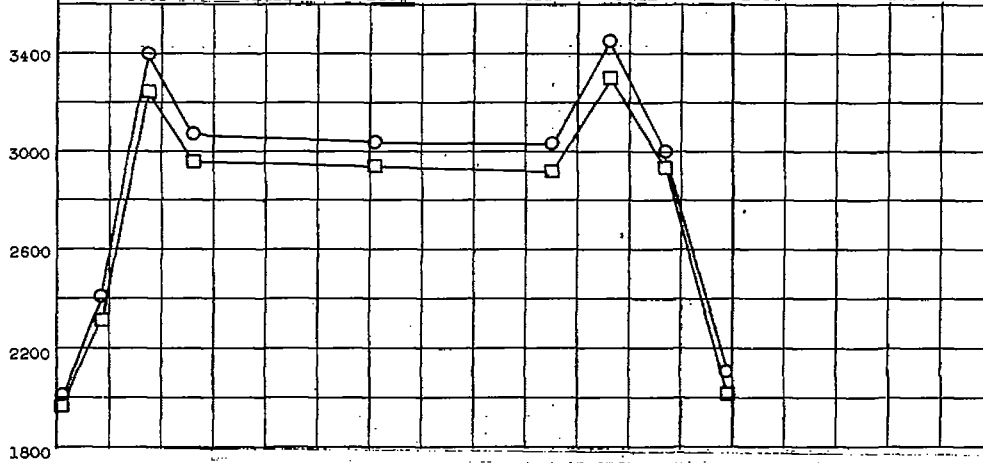
(a) Temperatures 1/4 inch from inside wall.



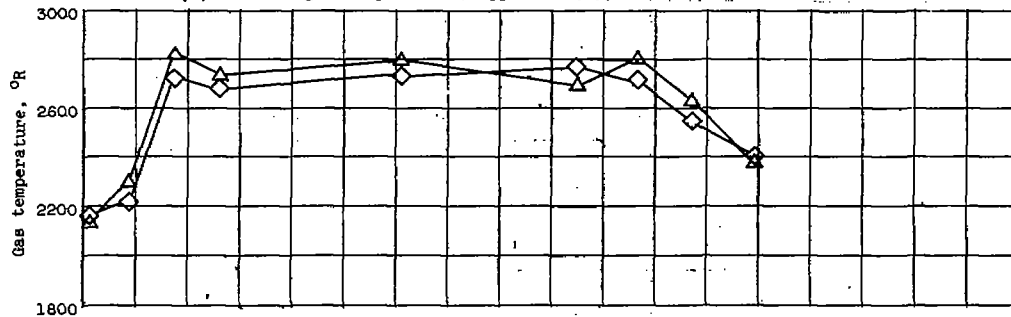
(b) Temperatures 1/2 inch from inside wall.

Figure 13. - Effect of combustion-gas mass flow on gas temperatures near inside wall for configuration A.

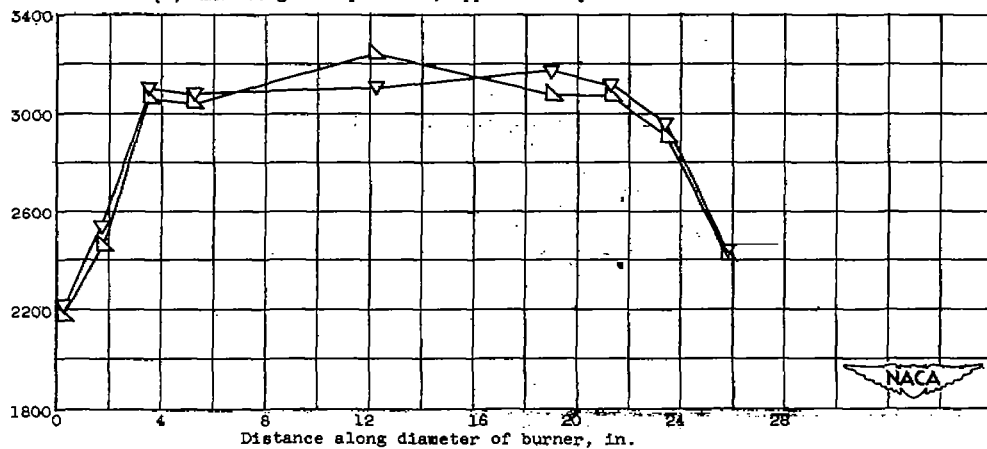
Exhaust-gas total temperature T_g (°R)	Mass-flow ratio W_a/W_g	Inlet cooling-air temperature $T_{a,B}$ (°R)	Tail-pipe fuel-air ratio f/a	Average inside-wall temperature T_w (°F)	Combustion-gas flow W_g (lb/sec)	Turbine-outlet total pressure (lb/sq ft-abs.)
2994	0.0672	541	0.0325	1198	21.89	1373
2858	.0814	550	.0315	1107	21.98	1350
3306	.1418	1340	.0363	1298	13.61	847
3272	.1415	548	.0385	1065	13.78	853
3425	.1411	771	.0450	1158	22.04	1394
3403	.1412	1408	.0444	1401	22.38	1409



(a) Exhaust-gas temperature, approximately 2926° R.



(b) Exhaust-gas temperature, approximately 3290° R.

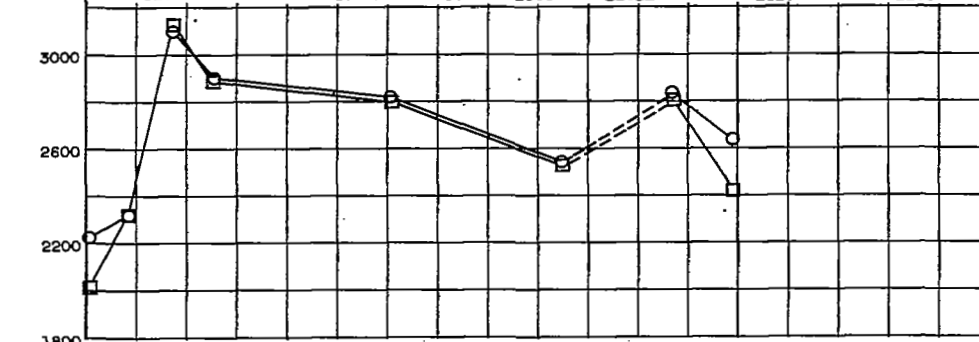


(c) Exhaust-gas temperature, approximately 3414° R.

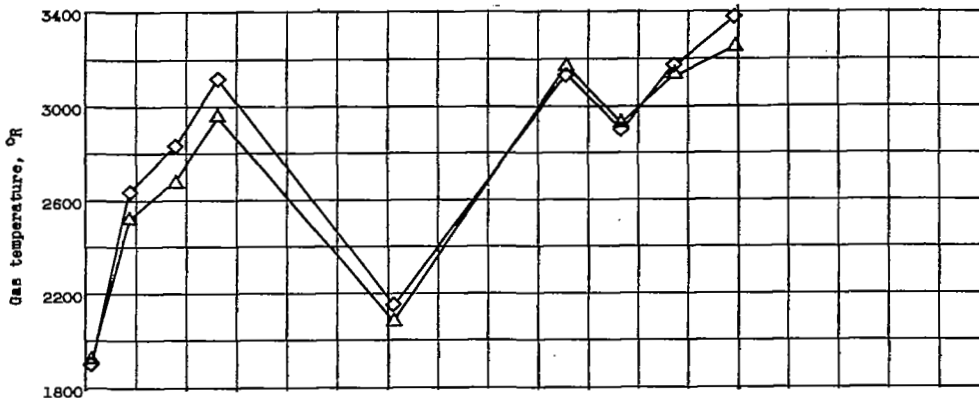
Figure 14. - Transverse profiles of combustion-gas temperature at station F, configuration A.

2408

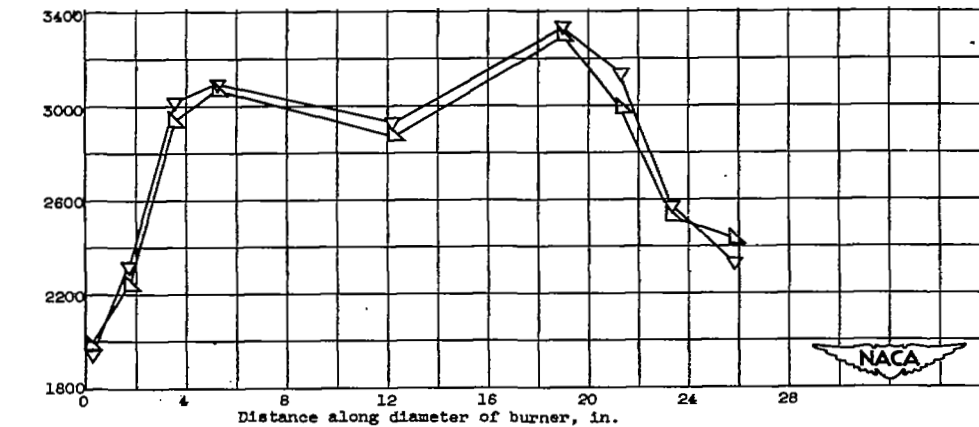
Exhaust-gas total temperature	Mass-flow ratio	Inlet cooling air temperature	Tail-pipe fuel-air ratio	Average inside-wall temperature	Combustion-gas flow	Turbine-outlet total pressure	Average gas temperature 1/4 in. from inside wall
T_g (°R)	W_g/W_a	$T_{a,B}$ (°R)	f/a	T_w (°F)	W_g (lb/sec)	(lb/sq ft abs.)	$T_{g,1/4}$ (°R)
3266	0.1430	534	0.0393	866	22.37		2448
3305	.1917	513	.0391	1164	22.01		2354
3215	.1449	495	.0409	1089	22.02	1416	2870
3214	.1422	500	.0599	999	22.23	1410	2840
3214	.1426	828	.0371	1096	22.37	1415	2099
3251	.1389	1040	.0370	1096	22.32	1419	2109



(a) Configuration A.



(b) Configuration B.



(c) Configuration C.

Figure 15. - Effect of fuel distribution on transverse profiles of combustion-gas temperature at station F.



2408

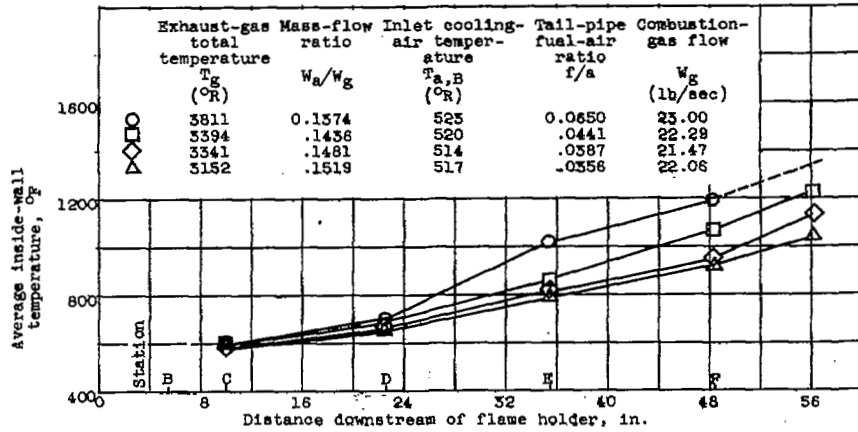


Figure 16. - Effect of exhaust-gas temperature on longitudinal profiles of average inside-wall temperature for configuration A.

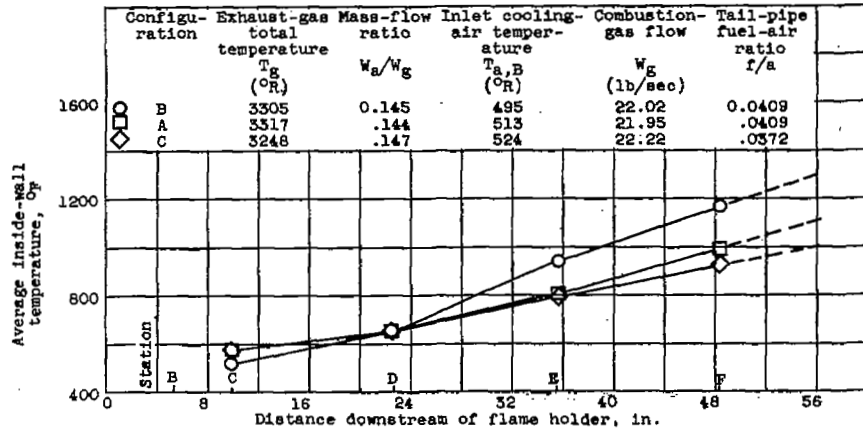


Figure 17. - Effect of fuel distribution on longitudinal profile of average inside-wall temperature.

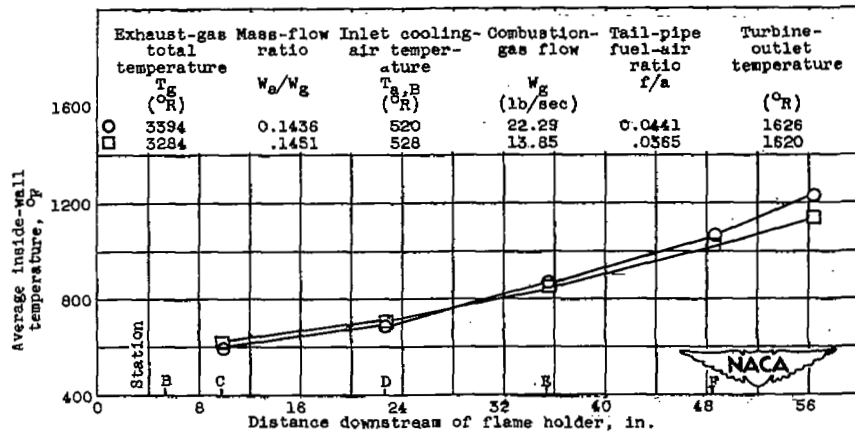


Figure 18. - Effect of combustion-gas mass flow on longitudinal profile of inside-wall temperature for configuration A.

2408

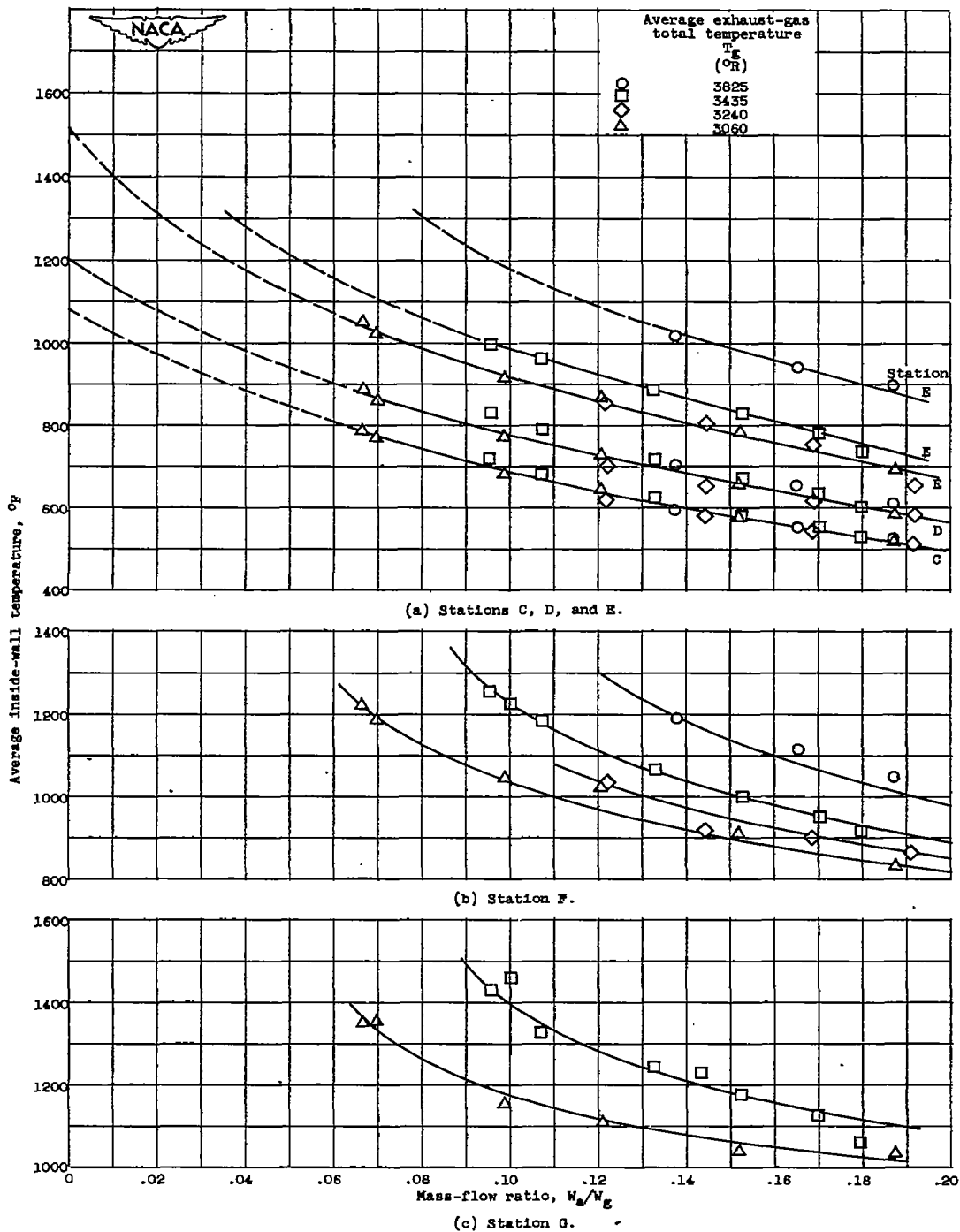
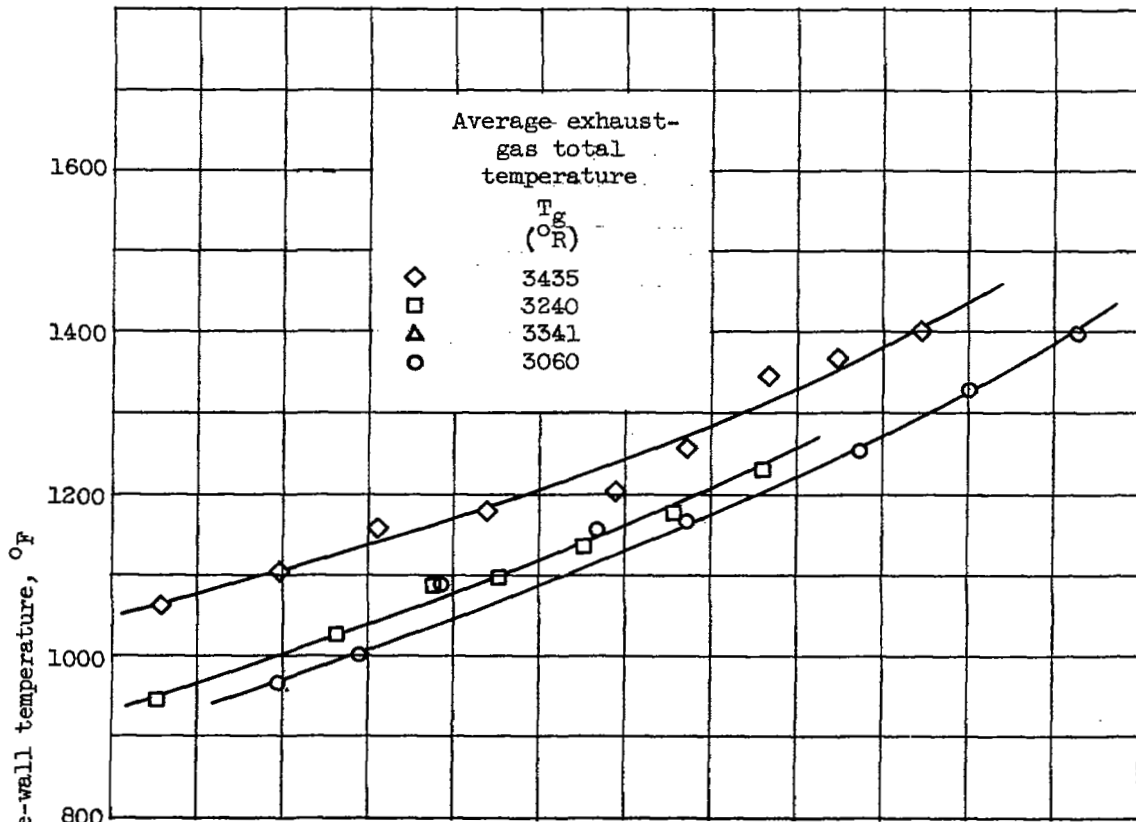
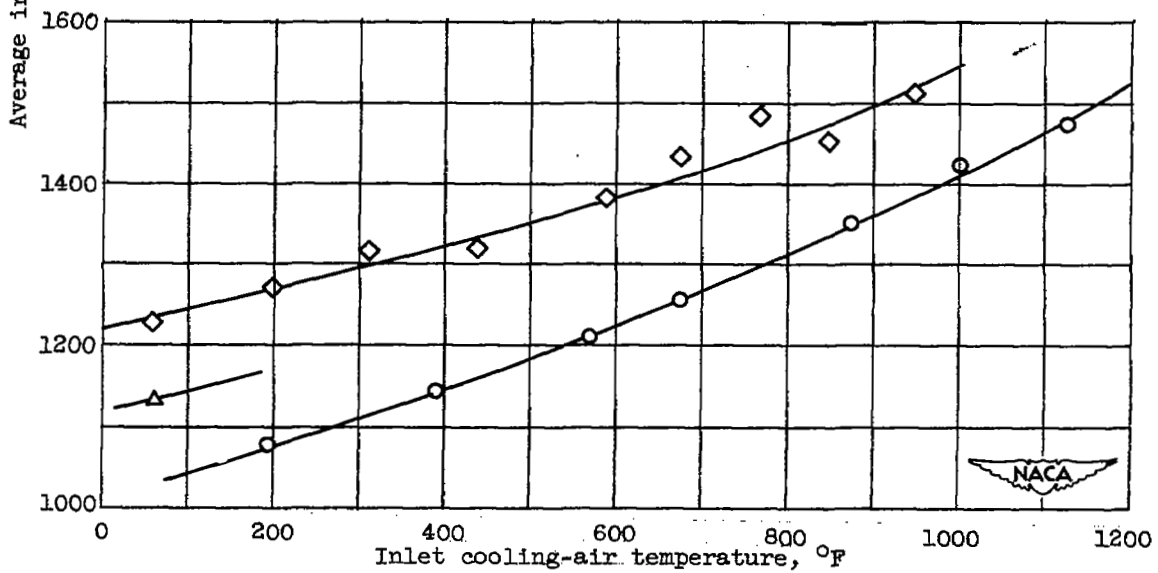


Figure 19. - Variation of average inside-wall temperature with mass-flow ratio of cooling air to combustion gas for configuration A. Approximate inlet cooling-air temperature, 520° R.

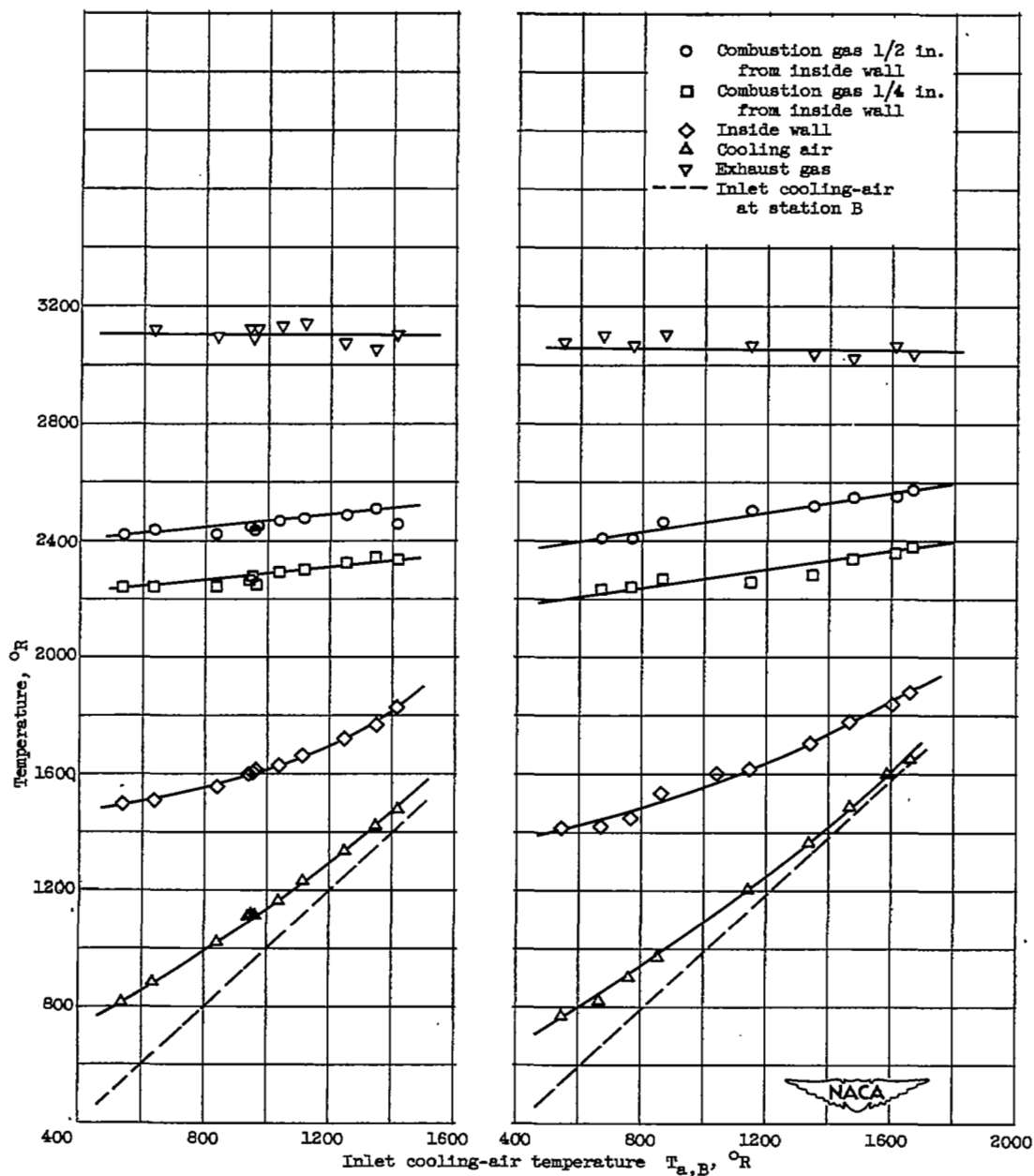


(a) Station F.



(b) Station G.

Figure 20. - Variation of inside-wall temperature with inlet cooling-air temperature for configuration A. Mass-flow ratio, 0.145.



(a) Configuration A; exhaust-gas temperature, 3064° R; combustion-gas flow, 22.3 pounds per second; mass-flow ratio, 0.098.

(b) Configuration A; exhaust-gas temperature, 3095° R; combustion-gas flow, 22.3 pounds per second; mass-flow ratio, 0.148.

Figure 21. - Relation of temperatures at station F.

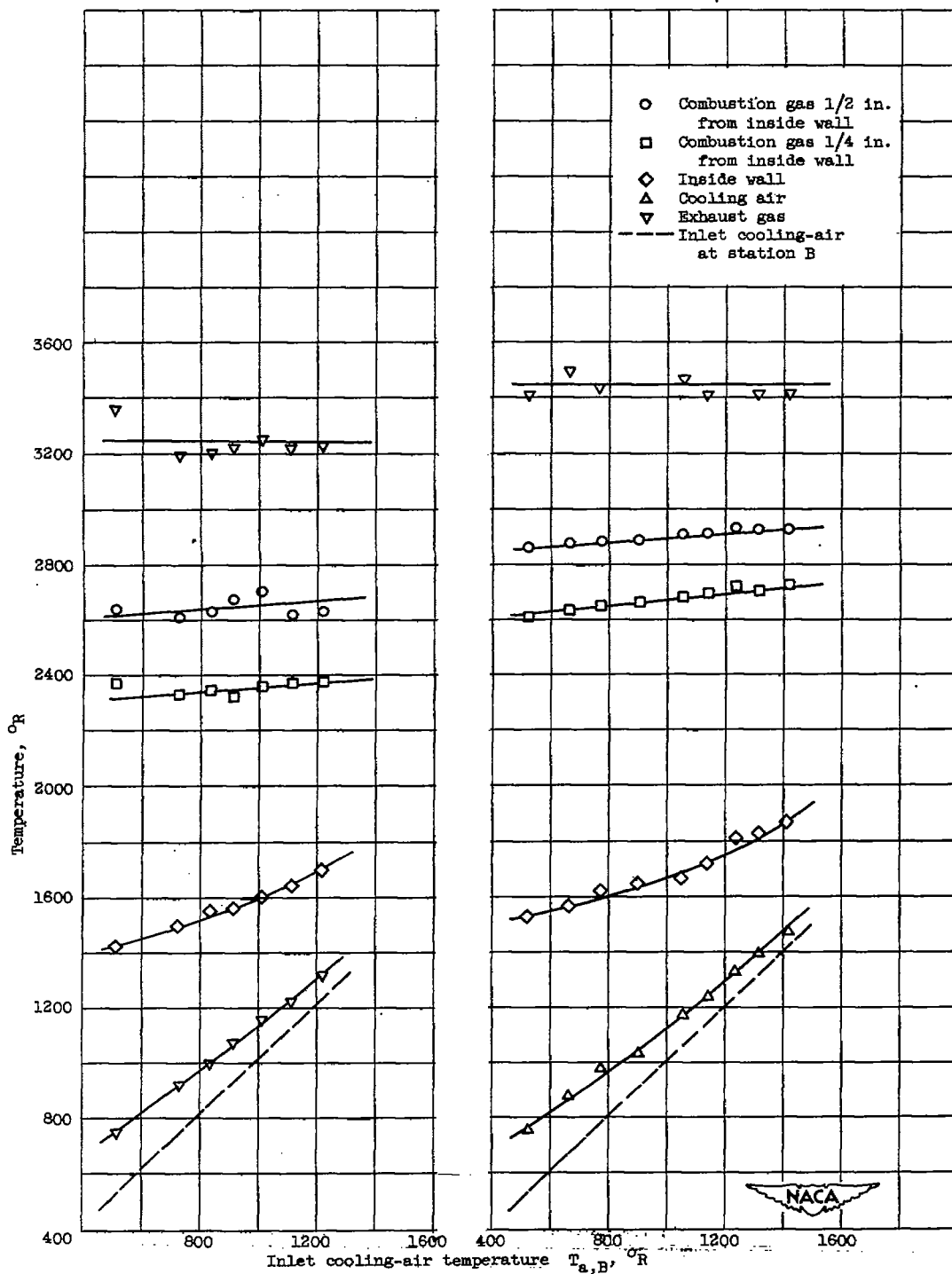


Figure 21. - Continued. Relation of temperatures at station F.

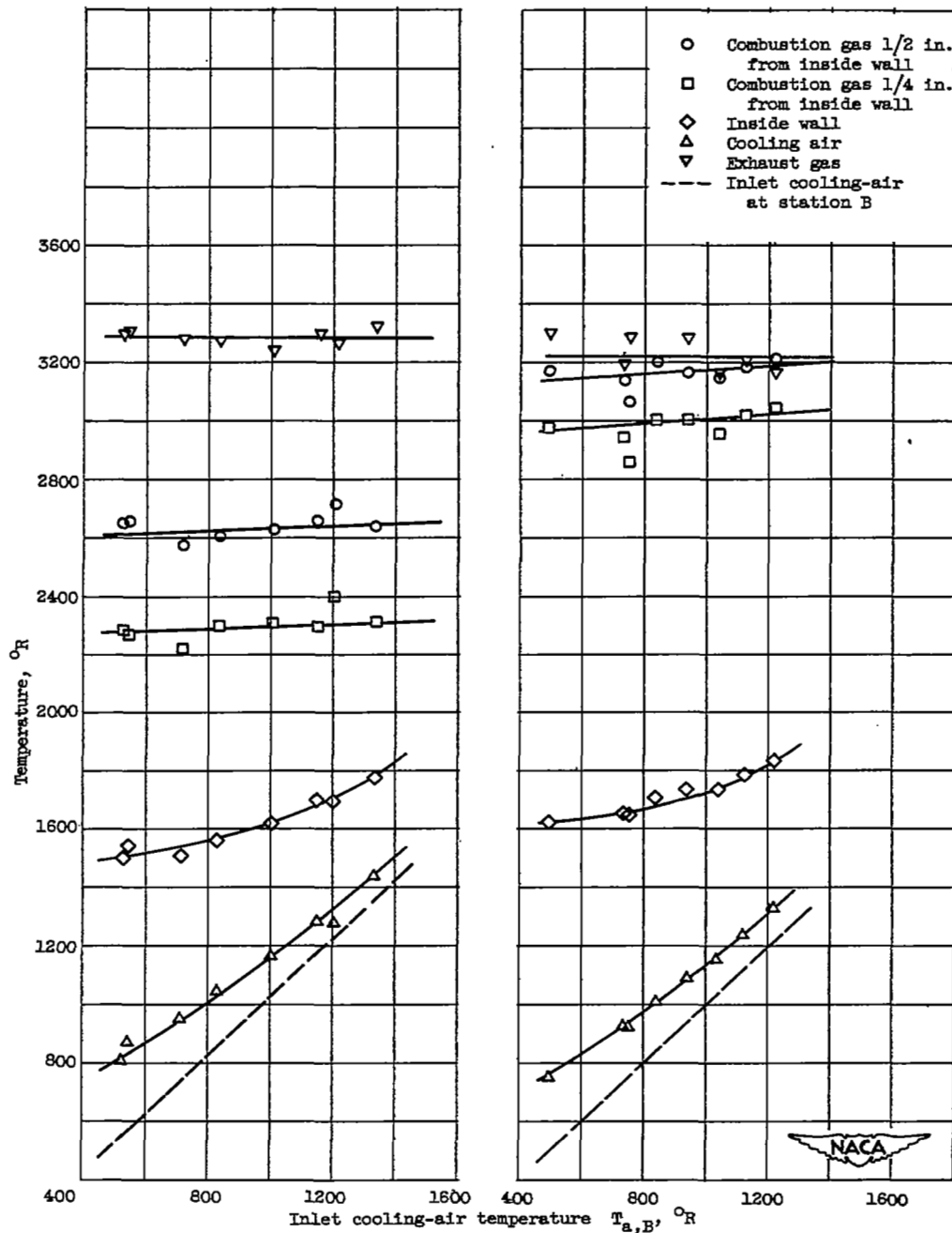
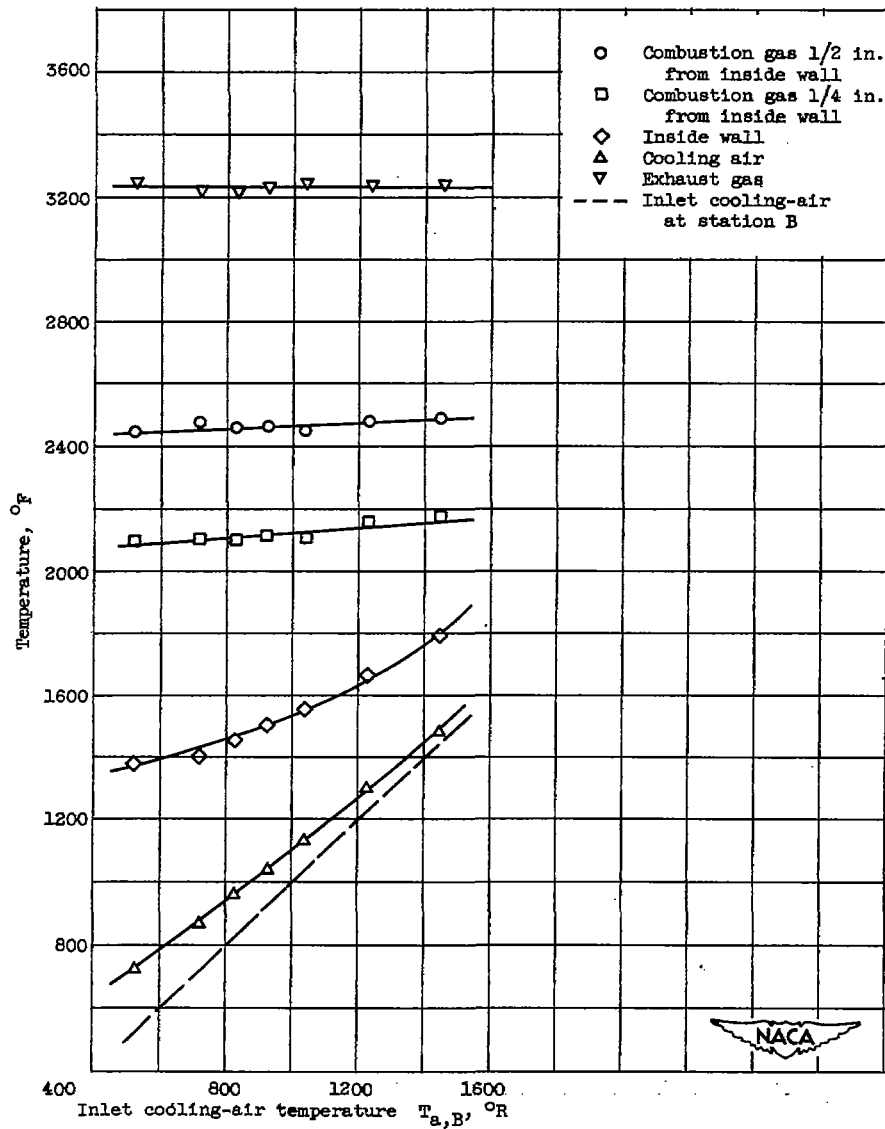


Figure 21. - Continued. Relation of temperatures at station F.



(g) Configuration C; exhaust-gas temperature, 3235° R; combustion-gas flow, 22.3 pounds per second; mass-flow ratio, 0.143.

Figure 21. - Concluded. Relation of temperatures at station F.

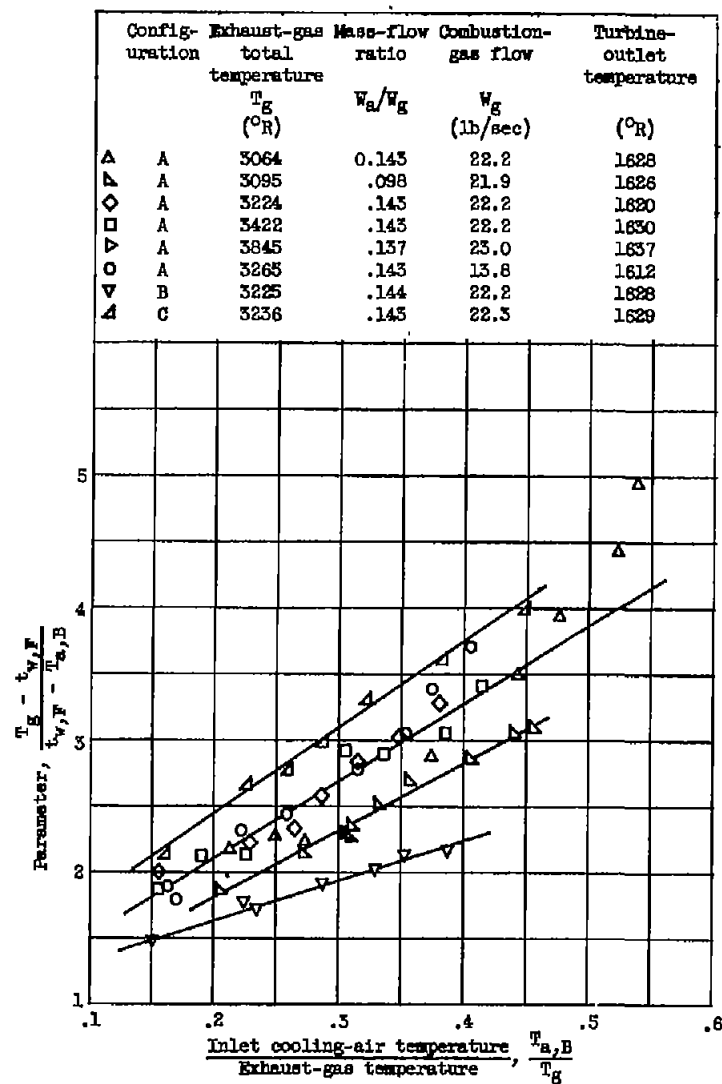


Figure 22. - Comparison of effects of exhaust-gas temperature level, radial distribution of tail-pipe fuel flow, and mass-flow ratio on cooling characteristics.

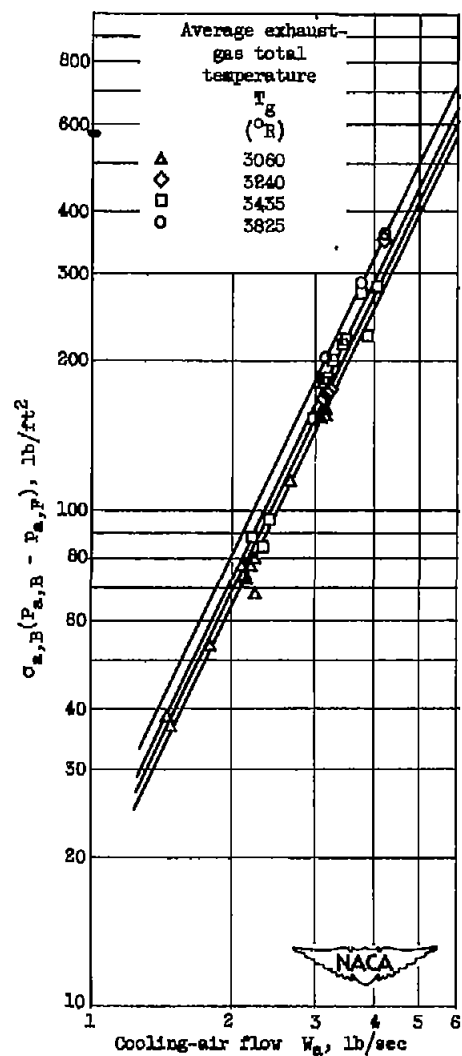


Figure 23. - Correlation of cooling-air pressure drop.

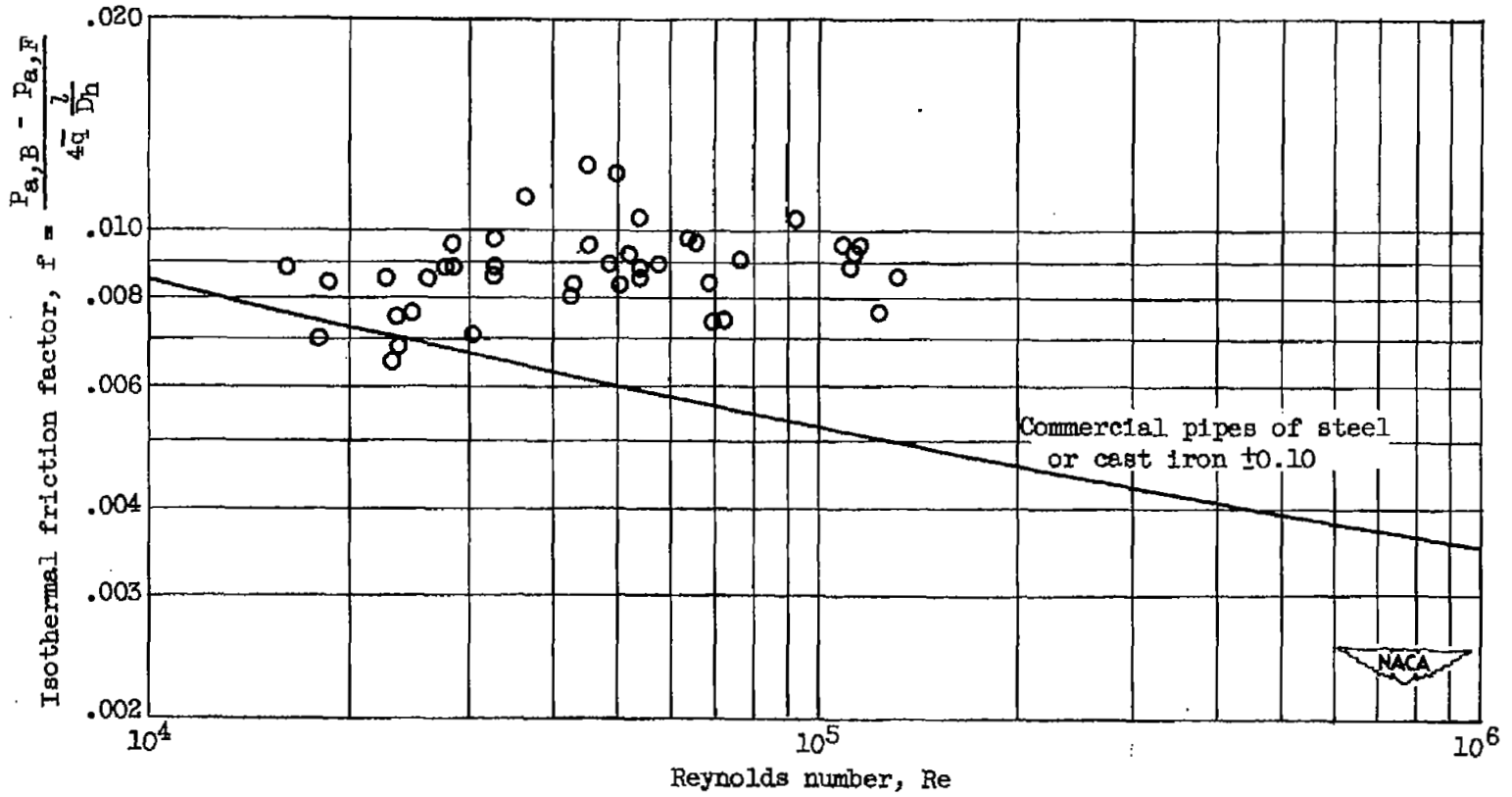


Figure 24. - Isothermal friction factor for instrumented cooling passages.

SECURITY INFORMATION

NASA Technical Library



3 1176 01434 9774

UNCLASSIFIED



UNCLASSIFIED